

1 **Variations in the chemical composition of the submicron aerosol and in the**
2 **sources of the organic fraction at a regional background site of the Po Valley**
3 **(Italy)**

4
5 **M. Bressi¹, F. Cavalli¹, C. A. Belis¹, J. -P. Putaud¹, R. Fröhlich², S. Martins dos Santos¹, E. Petralia³, A. S.**
6 **H. Prévôt², M. Berico³, A. Malaguti³ and F. Canonaco²**

7
8 ¹European Commission, Joint Research Centre, Institute for Environment and Sustainability, Air and
9 Climate Unit, Via Enrico Fermi 2749, Ispra (VA) 21027, Italy.

10 ²Paul Scherrer Institute, Laboratory of Atmospheric Chemistry, Villigen 5232, Switzerland.

11 ³Italian National Agency for New Technologies, Energy and Sustainable Economic Development (ENEA),
12 Via Martiri di Monte Sole 4, Bologna 40129, Italy.

13
14 Correspondence to:

15 michael.s.bressi@gmail.com, claudio.belis@jrc.ec.europa.eu, fabrizia.cavalli@jrc.ec.europa.eu

16
17 **Abstract**

18 Fine particulate matter (PM) levels and resulting impacts on human health are in the Po Valley (Italy)
19 among the highest in Europe. To build effective PM abatement strategies, it is necessary to characterize
20 fine PM chemical composition, sources and atmospheric processes on long time scales (>months), with
21 short time resolution (<day), and with particular emphasis on the predominant organic fraction. Although
22 previous studies have been conducted in this region, none of them addressed all these aspects together.
23 For the first time in the Po Valley, we investigate the chemical composition of non-refractory submicron
24 PM (NR-PM₁) with a time-resolution of 30 minutes at the regional background site of Ispra during one full
25 year, using an Aerosol Chemical Speciation Monitor (ACSM) under the most up-to-date and stringent
26 quality assurance protocol. The identification of the main components of the organic fraction is made
27 using the Multilinear-Engine 2 algorithm implemented within the latest version of the SoFi toolkit. In
28 addition, with a view of a potential implementation of ACSM measurements in European air quality
29 networks as a replacement of traditional filter-based techniques, parallel multiple off-line analyses were
30 carried out to assess the performance of the ACSM in the determination of PM chemical species regulated
31 by Air Quality Directives. The annual NR-PM₁ level monitored at the study site (14.2 µg/m³) is among the

32 highest in Europe, and is even comparable to levels reported in urban areas like New York City and Tokyo.
33 On the annual basis, submicron particles are primarily composed of organic aerosol (OA, 58% of NR-PM₁).
34 This fraction was apportioned into oxygenated OA (OOA, 66%), hydrocarbon-like OA (HOA, 11% of OA),
35 and biomass burning OA (BBOA, 23%). Among the primary sources of OA, biomass burning (23%) is thus
36 bigger than fossil fuel combustion (11%). Significant contributions of aged secondary organic aerosol
37 (OOA) are observed throughout the year. The unexpectedly high degree of oxygenation estimated during
38 wintertime is probably due to the contribution of secondary BBOA and the enhancement of aqueous
39 phase production of OOA during cold months. BBOA and nitrate are the only components of which
40 contributions increase with the NR-PM₁ levels. Therefore, biomass burning and NO_x emission reductions
41 would be particularly efficient in limiting submicron aerosol pollution events. Abatement strategies
42 conducted during cold seasons appear to be more efficient than annual-based policies. In a broader
43 context, further studies using high-time resolution analytical techniques on a long-term basis for the
44 characterization of fine aerosol should help better shape our future air quality policies, which constantly
45 need refinement.

46

47 1. Introduction

48 The Po Valley region - located in northern Italy - is amongst the most polluted areas in Europe (van
49 Donkelaar et al., 2010; EEA, 2013). Annual PM_{2.5} (particulate matter with an aerodynamic diameter below
50 2.5 µm) mean concentrations can significantly exceed the European PM_{2.5} annual limit value (25 µg/m³ in
51 2015, European Directive 2008/50/EC) and the recommendations of the World Health Organization (PM_{2.5}
52 annual average of 10 µg/m³; WHO, 2006) at urban (e.g. Bologna, 35.8 µg/m³) and regional background
53 sites (e.g. Ispra, 32.2 µg/m³; Putaud et al., 2010). Consequently, PM_{2.5} impacts on human health are among
54 the most severe in Europe (EC, 2005), while impacts on the local radiative forcing are substantial (Clerici
55 and Mélin, 2008; Ferrero et al., 2014; Putaud et al., 2014b). Effective PM abatement strategies are thus
56 needed in the Po Valley and require an in-depth knowledge of the chemical composition of fine PM, to
57 quantify its sources and the atmospheric processes leading to its secondary formation.

58 In this region, high levels of fine aerosol are mostly due to the conjunction of i) high pollutant
59 emissions related to industrial, transport, biomass burning and agricultural activities - the Po river basin
60 hosting 37% of the Italian industries, 55% of the livestock and contributing 35% of the Italian agricultural
61 production (WMO et al., 2012) - and ii) the specific geography and topography of this area - a flat basin
62 surrounded by the Alps and Apennine Mountains dominated by weak winds that favour the accumulation
63 of pollutants (Decesari et al., 2014; Kukkonen et al., 2005; Pernigotti et al., 2012). As a consequence, PM

64 levels are not only high in urban areas but also at regional and rural background sites, which are key
65 locations for investigating air pollution due to their distance from local sources and local phenomena.
66 Measurements of fine PM mass and chemical composition at rural background sites are in addition
67 specifically required in the current European Directive on air quality (EU, 2008).

68 Previous studies have investigated the properties of fine aerosols at regional and rural background
69 sites of the Po valley region, including their chemical characteristics (e.g. Carbone et al., 2014; Putaud et
70 al., 2002, 2010; Saarikoski et al., 2012), and their main sources (Belis et al., 2013; Gilardoni et al., 2011;
71 Larsen et al., 2012; Perrone et al., 2012). Fine aerosols are primarily made of organics (30-80% of fine PM
72 mass, depending on the site and season studied), followed by ammonium nitrate and ammonium sulfate.
73 Their main sources are fossil fuel, biomass burning and biogenic emissions to name a few. In addition,
74 studies based on aerosol mass spectrometer measurements have been conducted in the Po valley, with
75 the aim of characterizing specific phenomena (e.g. fog events, cooking aerosols) or seasons (Dall'Osto et
76 al., 2015; Decesari et al., 2014; Gilardoni et al., 2014; Saarikoski et al., 2012). In studies dealing with long
77 time-series (entire season or year), the chemical composition of fine aerosol is generally measured with a
78 relatively low time resolution (typically 24 hours), thus preventing from studying its diurnal variation and
79 short-lived chemical-physical processes. When documented with higher time-resolutions (1 hour or less),
80 aerosol chemical composition and their source are usually characterized for intensive campaigns of a few
81 weeks only, hence not suitable to depict the seasonal or yearly air quality situation. In addition, the
82 complexity of the fine organic fraction (e.g. Jimenez et al., 2009) requires state-of-the-art analytical and
83 source apportionment (SA) techniques to identify organic aerosol chemical properties and sources.

84 The recently developed Aerosol Chemical Speciation Monitor (ACSM, Aerodyne Research Inc., Ng
85 et al., 2011a) is suitable to fill these gaps by providing the chemical composition of non-refractory
86 submicron aerosols (NR-PM₁) with a time resolution of 30 min, while operating on long time scales. Even
87 though promising results have been recently reported (e.g. Budisulistiorini et al., 2014; Canonaco et al.,
88 2013, 2015; Minguillón et al., 2015; Ng et al., 2011a; Petit et al., 2015; Ripoll et al., 2015; Sun et al., 2012),
89 this technique is still novel and requires additional field deployment to test its consistency with
90 independent methods for the monitoring of fine PM chemistry (e.g. filter measurements). In addition,
91 information on the accuracy of this technique is of paramount importance given the growing number of
92 ACSMs in Europe and the necessity to build a network of quality assured and harmonized instruments for
93 comparability of results – at present about 20 ACSMs are in operation in Europe ([http://www.psi.ch/acsm-](http://www.psi.ch/acsm-stations/overview-full-period)
94 [stations/overview-full-period](http://www.psi.ch/acsm-stations/overview-full-period)) within the frame of the EU ACTRIS network (Aerosols, Clouds, and Traces
95 gases Research InfraStructure, <http://www.actris.eu/>). Moreover, by using receptor models, the

96 apportionment of organic aerosol (OA) into its major components - hydrocarbon-like (HOA), biomass
97 burning (BBOA) and oxygenated OA (OOA) - can be performed (Lanz et al., 2007; Zhang et al., 2011 and
98 references therein).

99 In this study, we used an ACSM during one year with a 30 min time-resolution at a regional
100 background site of the Po Valley and performed subsequent SA analyses with the aim of: i) describing the
101 high time resolved chemical composition of NR-PM₁ on a long time-scale, to better understand the
102 physicochemical processes driving its temporal variations, ii) apportioning the organic fraction into its
103 main sources, iii) identifying PM abatement strategies to efficiently reduce NR-PM₁ pollution events at
104 regional background areas of the Po valley, and iv) assessing the atmospheric consistency of ACSM
105 measurements when compared to independent analytical methods, to evaluate its possible
106 implementation in future European Air Quality networks.

107

108 2. Material and methods

109 2.1. Sampling site

110 Measurements were conducted at the European Commission – Joint Research Centre (EC-JRC) Ispra site
111 (45°48'N, 8°38'E, 217 m a.s.l.; Fig. S1), which is part of the European Monitoring and Evaluation
112 Programme (EMEP) measurement network ([http://www.nilu.no/projects/ccc/
113 sitedescriptions/it/index.html](http://www.nilu.no/projects/ccc/sitedescriptions/it/index.html)) and the Global Atmosphere Watch (GAW) regional stations
114 (<http://www.wmo.int/pages/prog/arep/gaw/measurements.html>). It is located on the northwest edge of
115 the Po Valley region, 60 km northwest of the Milan urban area. It can be regarded as a “regional/rural
116 background” site following the criteria recommended by the European Environment Agency (Larssen et
117 al., 1999). For simplicity, the term “regional background site” will be used in the following although
118 comparisons with rural background sites from other studies will also be reported. Further information on
119 the study site can be found in Putaud et al. (2014b).

120

121 2.2. Aerosol Chemical Speciation Monitor (ACSM)

122 The recently developed ACSM (Aerodyne Research Inc., ARI) was used to measure the non-refractory (NR)
123 chemical composition (organics, nitrate, sulfate, ammonium, chloride) of submicron particles (PM₁) with
124 a 30 minutes time resolution. The operating principle of the ACSM is similar to the widespread Aerodyne
125 aerosol mass spectrometer (Canagaratna et al., 2007; Jayne et al., 2000), with the difference that the
126 former does not inform on the size distribution of the chemical composition of NR-PM₁. A full description
127 of the ACSM can be found in Ng et al. (2011a). Briefly, an aerodynamic lens is used to focus submicron

128 particles (50% transmission range of 75-650 nm; Liu et al., 2007), which are then vaporized in high vacuum,
129 ionized by electron ionization (at 70eV) and detected by a quadrupole mass spectrometer (Pfeiffer
130 Vacuum Prisma Plus RGA). Two different quadrupole-ACSMs (Q-ACSMs) were used in this study (from
131 March 2013 to February 2014): Q-ACSM#1 from 01 March to 18 August 2013 and Q-ACSM#2 from 20 June
132 2013 to 28 February 2014. Note that Q-ACSM#2 was not running from 3 November to 18 December due
133 to its participation in the first inter-ACSM comparison exercise (Crenn et al., 2015). The reproducibility
134 and consistency with independent measurements are discussed in Sect. 3.1. In the following, orthogonal
135 regressions are reported unless otherwise stated.

136 Both ACSMs were operated with the latest Data Acquisition (DAQ 1.4.3.8 to 1.4.4.5) and Data
137 Analysis (DAS 1.5.3.0 to 1.5.3.2) software (ARI, <https://sites.google.com/site/ariacsm/mytemplate-sw>)
138 available at the time of use, which are developed within Igor Pro 6.32A (Wavemetrics). Recommendations
139 provided by Aerodyne (2010a, 2010b) and Ng et al. (2011a) were followed for the operation, calibration
140 and data analysis of the ACSMs. Ammonium nitrate calibrations were performed seasonally and used for
141 the determination of experimental nitrate response factors (RF) and ammonium relative ionization
142 efficiencies (RIE, see Sect. S1 for further details). Annual average and season-dependent experimental RF
143 and RIE values were alternatively applied to assess whether the ACSM is stable over multi-seasonal
144 periods (see Sect. 3.1 for results). Seasons are defined as spring (MAM), summer (JJA), autumn (SON) and
145 winter (DJF). RIEs for organics, nitrate and chloride (1.4, 1.1 and 1.3, respectively) were taken from the
146 literature (Canagaratna et al., 2007; Takegawa et al., 2005). RIE for sulfate was experimentally determined
147 based on ammonium sulfate calibrations for ACSM#2, and was taken from the literature for ACSM#1 (see
148 Sect. S1). Collection efficiencies (CE) set as i) a fixed 0.5 value (e.g. Budisulistiorini et al., 2013) or ii)
149 following the composition-dependent CE algorithm introduced by Middlebrook et al. (2012) were
150 compared in order to determine the most appropriate CEs (see Sect. 3.1 for results).

151

152 2.3. Additional analytical techniques

153 Additional measurements routinely performed at the JRC-Ispra site are used in this study (see Putaud et
154 al., 2014a for a full description). $PM_{2.5}$ are sampled on quartz fibre filters (Pall, 2500 QAT-UP) with a
155 Partisol PLUS 2025 sampler equipped with a carbon honeycomb denuder operating at 16.7 L/min from 01
156 March 2013 to 28 February 2014 with daily filter changes at 08:00 UTC. Major ions (NH_4^+ , K^+ , NO_3^- , SO_4^{2-} ,
157 etc.) are analysed by ion chromatography (Dionex DX 120 with electrochemical eluent suppression) after
158 extraction in Milli-Q water (Millipore). Organic and elemental carbon (OC and EC, respectively) are
159 quantified by a thermal-optical method (Sunset Dual-optical Lab Thermal-Optical Carbon Aerosol

160 Analyzer) using the EUSAAR-2 protocol (Cavalli et al., 2010). Equivalent black carbon (BC) is measured by
161 a Multi Angle Absorption Photometer (MAAP, Thermo Scientific, model 5012) applying an absorption
162 cross section of 6.6 m²/g of equivalent black carbon at the operation wavelength of 670 nm. Particle
163 volume concentrations are determined with a home-made Differential Mobility Particle Sizer (DMPS)
164 combining a Vienna-type Differential Mobility Analyser (DMA) and a Condensation Particle Counter (CPC,
165 TSI 3010), following the European Supersites for Atmospheric Aerosol Research (EUSAAR) specifications
166 for DMPS systems (Wiedensohler et al., 2012). Meteorological variables (temperature, pressure, relative
167 humidity, precipitation, wind speed and direction) are determined from a weather transmitter WXT510
168 (Vaisala, Finland). Solar radiation is measured by a CM11 pyranometer (Kipp and Zonen, The Netherlands).

169

170 2.4. Apportionment of the organic fraction

171 The organic fraction was apportioned using the Positive Matrix Factorization approach (PMF, Lanz et al.,
172 2007; Paatero and Tapper, 1994; Ulbrich et al., 2009; Zhang et al., 2011) by applying the Multilinear Engine
173 2 algorithm (ME-2, Paatero, 2000) implemented in the SoFi tool (v4.8, Canonaco et al., 2013; Crippa et al.,
174 2014). Details on the theory and application of PMF and ME-2 can be found in the aforementioned studies.
175 Briefly PMF aims at factorizing an initial X matrix (representing the temporal variation of *m/z* signals here)
176 into two F and G matrices (representing factor profiles and contributions, respectively) putting a
177 constraint of non-negativity on F and G matrices. Contrary to classical program used to resolve PMF (e.g.
178 PMF2, PMF3), ME-2 allows any element of the F and G matrices to be constrained with a certain degree
179 of freedom. This ME-2 approach has been typically used to constrain full factor profiles (e.g. Amato et al.,
180 2009; Crippa et al., 2014), specific elemental ratios (e.g. Sturtz et al., 2014) or specific species contribution
181 (e.g. Crawford et al., 2005) in a given factor profile.

182 In our study, ME-2 is applied with and without constraining factor profiles (FPs), using the so-
183 called α -value approach (Canonaco et al., 2013) in the former case, which can be described as follows:

$$184 (f_{k,j})_{\text{solution}} = (f_{k,j})_{\text{reference}} \pm \alpha \cdot (f_{k,j})_{\text{reference}} \quad (1)$$

185 where *k* and *j* are the indexes for the factors and the species, respectively, $f_{k,j}$ is the element (*k*, *j*) of the F
186 matrix, the index “solution” stands for the PMF user solution, “reference” for the reference profile and
187 “ α ” is a scalar defined between 0 and 1 (e.g. applying an α -value of 0.10 lets $\pm 10\%$ variability to our FP
188 solution with respect to the reference FP). Following Crippa et al. (2014), we perform a sequence of runs
189 with i) unconstrained PMF, ii) fixed HOA, iii) fixed HOA and BBOA, iv) fixed HOA, BBOA and cooking OA
190 (COA) factors before selecting the most appropriate solution. Uncertainties are calculated using the DAS
191 1.5.3.0 version following the methodologies of Allan et al., 2003a and Ulbrich et al. (2009). *m/z* 12 and 13

192 are removed for SA analysis since negative signals are observed most of the time. Reference factor profiles
193 (RFPs) are taken from ambient deconvolved spectra from the Aerosol Mass Spectrometry (AMS) spectral
194 database (Ulbrich et al., 2015). HOA and BBOA profiles are taken from Ng et al. (2011c) (average of profiles
195 from multiple studies) and COA from Crippa et al. (2013). Different α -values are tested (see Sect. 3.2)
196 applying i) relative standard deviations of averaged RFPs defined for every m/z (i.e. assuming that the
197 chosen averaged RFPs are representative of our data set), ii) recommendations of Crippa et al. (2014)
198 based on the SA of 25 European AMS data sets and iii) comparison with independent measurements (e.g.
199 NO_x, CO, BC, etc.). Solutions from 2 to 8 factors are investigated in order to choose the appropriate
200 number of factors (see Sect. S2 and 3.2).

201

202 3. Quality assurance / quality control

203 3.1. Quality assurance / quality control of ACSM measurements

204 Ammonium nitrate calibrations performed on each ACSM are shown in

205 Figure S2. RF_{NO_3} and RI_{NH_4} do not present significant seasonal variability - e.g. for ACSM#2 $RF_{NO_3}=4.7E-$
206 $11\pm0.2E-11$ A. $\mu g^{-1}.m^3$ - , suggesting constant calibration factors may be used throughout the campaign.

207 On the other hand, calibration factors exhibit substantial discrepancies between both ACSMs (e.g. RF_{NO_3}
208 of $2.5E-11$ and $4.7E-11$ A. $\mu g^{-1}.m^3$ for ACSM#1 and #2, respectively), suggesting that instrument-specific
209 factors are necessary. Applying constant and composition-dependent CEs does not lead to noticeable
210 differences (e.g. for NR-PM₁: $r^2=0.97$, slope= 1.00 ± 0.00 , y-intercept= 0.10 ± 0.03 $\mu g/m^3$, $n=14842$) due to i)
211 low sampling line RH (e.g. typically below 30% for ACSM#2), and ii) few high-nitrate-content events (only
212 5% of data exhibits ammonium nitrate mass fractions >40%, defined as high by Middlebrook et al., 2012).
213 The Middlebrook et al. (2012) algorithm is however preferred since slightly acidic aerosols are observed
214 at the study site (on average sulfate plus nitrate against ammonium in $\mu eq/m^3$: $r^2=0.96$, slope= 1.21 ± 0.00 ,
215 intercept= 0.01 ± 0.00 $\mu eq/m^3$, $n=14842$).

216 A comparison performed between the two ACSMs used in this study during a 2-month summer
217 period is shown in Figure S3. Very good correlations are observed for every chemical component
218 ($0.91 < r^2 < 0.98$, $n=1402$, hourly average) - chloride excluded - with slopes relatively close to one
219 ($0.87 < \text{slopes} < 1.42$), indicating a fairly good comparability between both instruments. One of the two
220 ACSM also participated in the first-ever inter-ACSM comparison exercise performed between 13 different
221 European Q-ACSMs during 3 weeks in Paris, France (Crenn et al., 2015). Satisfactory performances -
222 defined by $|z\text{-scores}| < 2$ - are reported for our instrument regarding every chemical component and NR-
223 PM₁ mass, attesting the consistency of our measurements with other European sites.

224 Measurements performed by the ACSM and independent off-line and on-line analytical
225 techniques are compared in Figure 1 and Table 1. An overall good agreement is found for every major
226 components throughout the year (typically $r^2 > 0.8$), although discrepancies are observable for specific
227 species and seasons. On the annual scale, a good agreement ($r^2 = 0.77$, $n = 317$) is found between organics
228 from ACSM and OC from filter measurements in spite of expected filter sampling artefacts (Maimone et
229 al., 2011; Turpin et al., 2000; Watson et al., 2009). Even better agreements are observed on a seasonal
230 basis ($r^2 \sim 0.9$), with steeper slopes in summer compared with winter, which likely reflects the different
231 degrees of oxygenation of organics among seasons (leading to different OM-to-OC ratios). However, these
232 slopes cannot be directly regarded as the OM-to-OC ratios due to i) differences in size fractions between
233 both methods (PM_{10} for ACSM and $PM_{2.5}$ for filter measurements) and ii) uncertainties related to RIE_{Org} for
234 ACSM measurements (Budisulistiorini et al., 2014; Ripoll et al., 2015). An estimation of the OM-to-OC ratio
235 for submicron organics applying the methodology described by Canagaratna et al. (2015) is discussed in
236 Sect. 4.2. Good correlations are observed for nitrate during all seasons ($r^2 > 0.9$) but summer ($r^2 = 0.5$), which
237 is most likely related to enhanced evaporative losses of ammonium nitrate from filter during the latter
238 season (Chow et al., 2005; Schaap et al., 2004). Slopes range from 0.9 to 1.4 - summer excluded - which is
239 comparable to what is reported elsewhere (Budisulistiorini et al., 2014; Crenn et al., 2015; Ripoll et al.,
240 2015). Very good correlations are observed for sulfate in every season ($r^2 = 0.9-1.0$) with slopes close to 1
241 (0.9-1.1, winter excluded), consistent with its presence in the submicronic size fraction and its low
242 volatility leading to the minimization of sampling artefacts. Note that discrepancies have been reported
243 when comparing sulfate measured by the ACSM (Petit et al., 2015) or the AMS (Zhang, 2005) with
244 independent measurements. Our results suggest that ammonium sulfate calibrations should be
245 performed to experimentally determine sulfate RIEs, which appear to be instrument-specific but stable
246 over several months. Although aerosols are slightly acidic on average at the study site, ammonium mostly
247 neutralizes nitrate and sulfate throughout the campaign and thus exhibits behaviour in between the two
248 latter compounds. Higher uncertainties are associated with chloride from filter quantification, resulting in
249 no agreement with ACSM measurements in summer when the concentrations are the lowest ($r^2 = 0.00$),
250 and fairly good agreement during the other seasons ($r^2 = 0.64-0.77$). The high slope observed for the
251 ACSM#1 (e.g. 2.1 during spring) compared to the fairly good slopes observed for ACSM#2 (0.7-1.1)
252 suggests that chloride RIE might be instrument-specific and require appropriate calibrations for its
253 accurate quantification (see also Riffault et al., 2013 on this topic).

254 The sum of NR- PM_{10} components and BC has been compared to the volume concentration of PM_{10} .
255 Good agreement is found between both variables ($r^2 > 0.8$) giving further confidence on the consistency of

256 our ACSM measurements. The annual average particle density estimated from this comparison (i.e. slope)
257 is 1.6, which is typical of ambient aerosol particles densities (1.5-1.9 in Hand and Kreidenweis, 2002; Hu
258 et al., 2012; McMurry et al., 2002; Pitz et al., 2003, 2008). The higher densities observed during spring and
259 summer (1.9-2.0) than autumn and winter (1.3-1.5) are likely due to the enhanced contribution of
260 secondary aerosol and aged particles during the former period (Pitz et al., 2008).

261

262 3.2. Quality assurance / quality control of organic source apportionment

263 First, during the aforementioned inter-ACSM comparison study (Crenn et al., 2015), source
264 apportionment of organics was performed based on data from 13 Q-ACSMs (Fröhlich et al., 2015),
265 including one ACSM used in the present study. Satisfactory performances ($|z\text{-scores}| < 2$) are reported for
266 our ACSM using a similar approach as adopted in this study. This result demonstrates that our instrument
267 and the associated data treatment, including the source apportionment modelling, are capable of
268 accurately identifying and quantifying OA sources.

269

270 3.2.1. Model configurations

271 Regarding our specific study, the configuration applied to reach the optimal SA of organics is
272 thoroughly discussed in Sect. S2 (constrained factor profiles, number of factors, α -values and integration-
273 period durations). Briefly, constraining both HOA and BBOA factors result in satisfactory solutions with
274 relevant factor profiles, time series and daily cycles. Other configurations (e.g. unconstrained factors) lead
275 to unsatisfactory results with high seed variability, mixing of factors or absence of key fragments in
276 identified profiles (e.g. absence of m/z 43 and 44 in BBOA contrary to what is reported in Heringa et al.,
277 2011, Figure S4). Solutions applying different number of factors are investigated. Three-factors (HOA,
278 BBOA and OOA) are retained during spring, autumn and winter whereas two factors (HOA and OOA) are
279 most suitable during summer. A lower number of factors results in a mixing of them, whereas a higher
280 number generates additional factors - e.g. semi-volatile OOA (SV-OOA) during summer, OOA-BBOA during
281 autumn - which are not satisfactory - e.g. missing fragments or poor correlations with external data, see
282 Table S1. BBOA cannot be clearly identified during summer i.e. in this season agricultural waste burning
283 contributions are estimated to be minor (maximum 3-4% of OA, Sect. S2). Note that COA could not be
284 evidenced, likely due to the type of site studied (regional background) and the lower sensitivity, time- and
285 mass-to-charge-resolution of the ACSM compared to classical AMS instruments (further discussed in Sect.
286 S2; see also Dall'Osto et al., 2015 on this subject). Uncertainties associated with factor contributions are
287 estimated by performing sensitivity tests on α -values, which are regarded as the most subjective input

288 parameters. Five scenarios putting very low to very high constraints on the reference factor profiles have
289 been defined (see Table S2). Comparable solutions in terms of relative contributions (Figure S5) and
290 agreement with independent measurements (Table S2) are found when applying low to high constraints
291 following the empiric recommendations of Crippa et al. (2014). Unsatisfactory solutions are generally
292 reached under the extreme scenarios (fully fixed factor profiles and m/z specific standard deviations of
293 reference factor profiles). We decided to apply low constraints (i.e. α -values of 0.1 and 0.5 for HOA and
294 BBOA, respectively) to let as much freedom as possible to our factor profiles while remaining in the range
295 of plausible solutions. SA was performed on 3-months, 6-months and 1-year datasets. Although
296 comparable solutions are found for each configuration (number of factors, factor profiles, diurnal cycles,
297 comparisons with external data), applying SA on seasonal datasets was preferred since i) the seasonal
298 variability of factor profiles is captured and ii) questionable results are observed in summer for 6-months
299 and 1-year configurations (see Sect. S2). When comparing the sum of OA factor concentrations and
300 measured OA on the annual scale, OA is very well modelled ($r^2=0.97$, slope= 0.98 ± 0.00 , intercept= 0.1 ± 0.0
301 $\mu\text{g}/\text{m}^3$, $n=14842$).

302

303 3.2.2. Model optimal solution

304 Factor profiles, contributions and daily cycles of the optimal SA solution are presented in Figure
305 2. Independent factor profiles and time series are found for each season, which is a prerequisite for having
306 reliable SA solutions. HOA is identified during every season and exhibits a profile dominated by alkyl
307 fragments such as m/z 55 (from the $\text{C}_n\text{H}_{2n-1}^+$ ion series) and m/z 57 (from $\text{C}_n\text{H}_{2n+1}^+$ ion series; Ng et al.,
308 2011c). Its relative contribution is characteristic of traffic emissions, exhibiting a peak in the morning, and
309 higher contributions during weekdays than weekends (e.g. averages of 14 and 9%, respectively, in
310 autumn, Fig. S6). BBOA is found during every season except summer and has a profile similar to that of
311 HOA, except for the high contribution of m/z 60 ($\text{C}_2\text{H}_4\text{O}_2^+$) and 73 ($\text{C}_3\text{H}_5\text{O}_2^+$), which have been suggested
312 as biomass burning markers (Lee et al., 2010 and references therein). A distinct daily cycle with higher
313 contributions during night-time than daytime is observed, in addition to higher contributions during
314 weekends than weekdays (e.g. averages of 24 and 21%, respectively, in spring, Fig. S6), consistent with
315 residential heating emissions. The low BBOA concentrations modelled during late spring and early
316 autumn, as well as the small increased contribution observed during the morning also suggest residential
317 heating emissions. OOA is identified thanks to the predominant contribution of m/z 44 (CO_2^+) and 43
318 ($\text{C}_2\text{H}_3\text{O}^+$). The higher contribution of f_{44} (defined as m/z 44 to total organic signal; 0.17-0.23 depending on
319 seasons) with respect to f_{43} (defined similarly; 0.05-0.09) suggests that this OOA factor is highly oxidized

320 and presents low volatility (LV-) rather than semi-volatility (SV-) OOA characteristics (see Jimenez et al.,
321 2009 and Zhang et al., 2011 for definitions of these components). This statement is supported by very
322 good correlations ($r^2=0.96-0.99$) found between our unconstrained OOA profiles and the average low-
323 volatility OOA (LV-OOA) profile reported by Ng et al. (2011c) from 6 AMS studies. Interestingly, our OOA
324 profiles present slight seasonal differences that likely reflect changes in source contributions and/or
325 physical-chemical processes in this factor. For instance, f_{60} in OOA profiles is enhanced in winter (0.014)
326 compared with other seasons (0.001-0.004), which suggests that biomass burning contributes to this
327 factor during the aforementioned season, consistent with different studies reporting f_{60} in secondary OA
328 from biomass burning (e.g. Cubison et al., 2011; Heringa et al., 2011; see Sect. S2). Note that the mass
329 spectral resemblance of primary humic-like substances to LV-OOA might also partly explain this
330 observation (e.g. Young et al., 2015), i.e. that a small fraction of primary OA is found in this factor. Daily
331 cycles are comparable for all seasons with a bimodal pattern characterized by a small peak during night-
332 time and a prominent peak during daytime. The latter peak suggests that a fraction of (LV-) OOA could be
333 locally rather than regionally produced on the time scale of few hours only, likely due to enhanced
334 photochemical activities during daytime. The former peak could be due to i) the condensation of highly
335 oxygenated semi-volatile material favoured by night-time thermodynamic conditions or ii) a contribution
336 of SV-OOA in our OOA factor, which is generally dominated by LV-OOA. The absence of an f_{44} night-time
337 peak (Sect. 4.2) suggests that the second assumption is more probable implying that both SV-OOA and
338 LV-OOA influence our OOA factor.

339

340 3.2.3. Time series comparisons

341 Comparisons between our OA factors, m/z tracer and independent species time series are shown
342 in Table 2. OOA time series show very good agreement with Org_43 (organic signal at m/z 43) and Org_44
343 ($r^2>0.8$ and 0.9 , respectively) and relatively good agreement with secondary inorganic species (e.g. $r^2\geq 0.5$
344 for ammonium), indicating that this factor can be regarded as a surrogate for secondary organic aerosols.
345 Comparisons with sulfate (a low-volatility species) and nitrate (a semi-volatile species) confirm that our
346 OOA factor might be a mix of SV- and LV-OOA, since better agreement is found with one or the other
347 compound depending on the season studied. BBOA exhibits very good coefficients of determination when
348 compared with its presumable fragment tracers Org_60 and Org_73 ($r^2>0.97$), giving further confidence
349 on its appropriate quantification. Good correlations are generally found between BBOA and BC ($r^2\geq 0.5$,
350 except for summer) indicating that a large proportion of BC stems from biomass burning, consistent with
351 previous findings at the study site (Gilardoni et al., 2011, from EC measurements). A good agreement is

352 also observed with CO ($r^2 \geq 0.7$), as already reported in the Alpine valleys (e.g. Gaeggeler et al., 2008). HOA
353 is not as well correlated with external data or specific m/z , which could be related to i) the absence of
354 clear m/z tracers for this factor due to similarities with BBOA profile, ii) the absence of clear external
355 tracers due to co-emissions by fossil fuel and biomass burning activities of BC, CO and NO_x and iii) possible
356 uncertainties associated with the apportionment between HOA and BBOA. The first two assumptions are
357 supported by the better agreement observed between HOA and m/z fragments or independent data
358 during summer (e.g. $r^2=0.52$, $n=2208$ between HOA and BC) and specific months (e.g. May, September),
359 when biomass burning contributions are negligible. Although uncertainties associated with the accurate
360 apportionment of HOA and BBOA cannot be excluded (e.g. due to rotational ambiguity), several factors
361 evidence the robustness of the results and indicate that a mixing of both factors is unlikely, since HOA and
362 BBOA present i) independent factor time series during all seasons ($r^2=0.1-0.2$), ii) distinct and relevant
363 daily cycles and iii) no significant α -value variability.

364

365 4. Results and discussion

366 The meteorological representativeness of this one-year measurement is assessed by comparing the solar
367 irradiation, precipitation, and temperature monthly averages to the ones measured during 1990-2010 at
368 the study site (Figure S7). Comparable seasonal averages are generally found in our study and during the
369 bi-decadal reference period. Nevertheless compared to 1990-2010, Spring 2013 was rainier, Summer 2013
370 slightly warmer and sunnier, and Winter 2013-2014 rainier. Further information regarding the
371 representativeness of measurements performed at the study site during the year 2013 can be found in
372 Putaud et al. (2014a).

373

374 4.1. Chemical composition of NR-PM₁

375 An overview of the chemical composition of NR-PM₁ retrieved during this campaign is shown in Figure 3.
376 The annual averaged NR-PM₁ mass reported here ($14.2 \mu\text{g}/\text{m}^3$) ranges amongst the highest NR-PM₁ levels
377 (7th out of 41 sites) reported at rural and urban downwind sites in Europe (Crippa et al., 2014) and
378 worldwide (Jimenez et al., 2009; Zhang et al., 2007, 2011). Please note that these previous studies are
379 based on typically one month of measurements in different seasons. It is comparable to NR-PM₁ levels
380 reported during specific campaigns in the urban areas of New York City (USA, $12 \mu\text{g}/\text{m}^3$, Weimer et al.,
381 2006), Tokyo (Japan, $12-15 \mu\text{g}/\text{m}^3$, Takegawa et al., 2006) or Manchester (UK, $14 \mu\text{g}/\text{m}^3$, Allan et al., 2003a,
382 2003b). Our annual average NR-PM₁ mass is higher than the $10 \mu\text{g}/\text{m}^3$ guidelines given by the World
383 Health Organization for the annual average PM_{2.5} mass (including refractory and non-refractory

384 compounds; WHO, 2006). After similar conclusions have been drawn for PM_{2.5} and PM₁₀ size fractions
385 (Putaud et al., 2010), the Po Valley appears to be one of the most polluted regions in Europe with regard
386 to NR-PM₁ levels this time. Submicron aerosol particles are mostly made of organics (58%), nitrate (21%),
387 sulfate (12%) and ammonium (8%; Figure 3). The predominance of organics is typical of urban downwind
388 sites (e.g. average of 52% reported in Zhang et al., 2011). On the other hand, the noticeable proportion of
389 nitrate is characteristic of urban sites (18% in Zhang et al., 2011), which likely reflects the substantial
390 influence of anthropogenic activities emissions at our regional site. As a result, sulfate exhibits particularly
391 low contributions at the study site compared with other locations (generally >20% in Zhang et al., 2011).

392 NR-PM₁ levels present a clear seasonality with higher levels during spring (~18 µg/m³) and winter
393 (~15 µg/m³) compared with summer and autumn (~12 µg/m³). Higher levels were expected during cold
394 months due to enhanced biomass burning emissions and lower boundary layer heights (BLH), as
395 previously observed at the study site (Putaud et al., 2013). Expected seasonal variations of the chemical
396 composition of NR-PM₁ are observed, with i) higher nitrate contributions during the cold season which
397 favours its partitioning in the condensed phase (Clegg et al., 1998), ii) higher sulfate contributions during
398 summer, which can e.g. be associated with enhanced photochemical production (Seinfeld and Pandis,
399 2006) and lower amount of rainout (Fig. S7), and iii) relatively stable contributions for ammonium (mainly
400 neutralizing the two previous species) and organics (discussed later on).

401 A focus will now be made on daily cycles of the chemical composition of NR-PM₁ (Figure 4),
402 displayed for the first time during the 4 seasons in the Po Valley, thanks to the high time resolution and
403 stability of the ACSM. On the annual scale, daily cycles of NR-PM₁ levels are characterized by significantly
404 higher concentrations during night time than daytime, likely due to lower BLH, higher wood burning
405 emissions (during cold seasons) and lower temperatures favouring the partitioning of semi-volatile
406 inorganic (mainly ammonium nitrate) and organic material in the condensed phase, to name a few. A
407 distinct peak is however observed around noon, probably caused by enhanced photochemical production
408 of secondary organic compounds, and increased BLH favouring downward mixing of advected pollution,
409 especially during summer (Figure 4; Decesari et al., 2014). Note that this annual daily pattern is the
410 combination of distinct daily cycles varying with the season studied (Figure 4). In terms of relative chemical
411 composition, organics are dominating NR-PM₁ mass independently of the time of the day, with median
412 contributions ranging from ~60 to 70%. Nitrate exhibits higher contribution during night time due to its
413 abovementioned semi-volatile nature. Sulfate shows unexpected daily cycles with significantly different
414 (99.99% confidence level) relative contributions - and absolute concentrations - during daytime (~15% of
415 NR-PM₁ mass around noon) compared to night time (~10% around midnight, Figure 4), although its

416 formation was expected to occur mainly over longer time scales (i.e. days) in cloud droplets (Ervens et al.,
417 2011). This observation could be due to i) local production of sulfate with increased photochemical
418 production around noon at the study site and/or ii) diurnal changes of the atmospheric stratification in
419 the Po Valley as described by Saarikoski et al. (2012) and Decesari et al. (2014), enhancing aged particle
420 contribution during the middle of the day and the afternoon. Non-refractory chloride (mostly NH_4Cl ,
421 Huang et al., 2010) exhibits very low contributions independently of the hour of the day (medians below
422 0.5% of NR-PM_{10} mass) with however a slight increase at night, which is likely due to its presumable semi-
423 volatile nature here.

424

425 4.2. Focus on organic aerosols

426 An overview of the contribution of HOA, BBOA and OOA to OA is shown in Figure 5. On the annual average,
427 the organic fraction is dominated by the secondary component (OOA, 66%). Although this OOA
428 contribution is substantial, higher proportions are generally reported at rural and urban downwind sites
429 worldwide (90 and 82% of OA on average, respectively, Zhang et al., 2011). This lower relative contribution
430 of OOA is related to the higher contribution of (primary) BBOA in our study (23% of OA on the annual
431 average) compared to the previous ones. Considerable contributions of BBOA are explained by the specific
432 location of the study site in the vicinity of the Alps, where biomass burning is a major contributor to OA
433 (Belis et al., 2011; Herich et al., 2014; Lanz et al., 2010). Biomass burning emissions hence substantially
434 affect OA levels on the annual scale here. The contribution of HOA is comparatively smaller (11%),
435 indicating that despite the expected large contributions of fossil fuel emissions (i.e. traffic and industrial
436 emissions), those are not the major sources of primary OA at the study site. On the other hand, it is likely
437 that fossil fuel emissions of volatile organic compounds (VOCs) - which are OOA precursors - contribute
438 to our OOA levels as reported elsewhere (Gentner et al., 2012; Volkamer et al., 2006). At the study site,
439 Gilardoni et al. (2011) previously estimated on the basis of ^{14}C analyses that secondary organic carbon
440 stemming from fossil emissions might represent 12% of OC on the annual average. In other words, fossil
441 fuel emissions could represent approximately a quarter (12+11=23%) of total OA mass when both primary
442 and secondary OA fractions are accounted for. The analysis of the components' seasonal variations show
443 relatively stable HOA contributions (9-14%), higher contributions of BBOA during cold seasons due to
444 residential heating (up to 36% of OA on average during winter) and higher OOA contributions during
445 summer related to enhanced photochemical production (86% of OA on average).

446 OA can be further characterized investigating specific organic fragments. m/z 44 (mainly CO_2^+)
447 and 43 (mainly $\text{C}_2\text{H}_3\text{O}^+$) signals give insights on the nature of OA, as the former is primarily related to acids

448 or acid-derived species whereas the latter is mostly associated with non-acid oxygenates (Duplissy et al.,
 449 2011; Ng et al., 2011b). Daily variations of both f_{44} and f_{43} are shown in Figure 6, along with other major
 450 organic fragments. On average, f_{44} is predominant with respect to f_{43} (15 and 7%, respectively), which
 451 indicates that acid species dominate the OA composition with respect to non-acid oxygenates. Both
 452 fragments present different daily patterns underlying distinct mechanisms of formation. Acids'
 453 contributions are enhanced during daytime, which could be explained by photochemical processes and/or
 454 daily BLH variations as already discussed for sulfate. Non-acid oxygenates exhibit higher contributions
 455 during night time than daytime. This pattern could be due to i) the formation of semi-volatile non-acids
 456 during night time by e.g. condensation (Lanz et al., 2007), ii) their degradation during daytime by e.g.
 457 fragmentation reactions (Daumit et al., 2013) and/or iii) their conversion into acid-related species during
 458 daytime by e.g. functionalization or oligomerization reactions (Daumit et al., 2013). It should be specified
 459 that the enhancement of f_{44} during daytime and the decreasing of f_{43} during night-time only represent a
 460 small fraction of their total contributions to OA (Figure 6), suggesting that most acid and non-acid
 461 oxygenates have been formed before reaching our sampling site, i.e. have been imported from other
 462 regions. The other major OA fragments (m/z 29, 55, 57 and 60) present i) constant contributions for f_{29}
 463 due its various emission sources (HOA, BBOA, OOA; Ng et al., 2011c), ii) the absence of lunch peak for f_{55}
 464 (and also for the absolute contributions of m/z 55) consistent with the presumable low influence of
 465 cooking emissions, iii) morning and evening peaks for f_{57} characteristics of fossil fuel emissions and iv)
 466 higher contributions during night time for f_{60} in agreement with its biomass burning origin.

467 Using f_{43} and f_{44} , the oxygen-to-carbon (O/C), OM-to-OC (OM/OC), hydrogen-to-carbon (H/C)
 468 ratios and the carbon oxidation state (OSc) have been estimated for total OA based on the methodologies
 469 described by Aiken et al. (2008), Kroll et al. (2011) and Ng et al. (2011b), and applying the parameterization
 470 defined in Canagaratna et al. (2015), which can be summarized as follows:

$$471 \text{ O/C} = 4.31 f_{44} + 0.079 \quad (1)$$

$$472 \text{ OM/OC} = 1.28 \text{ O/C} + 1.17 \quad (2)$$

$$473 \text{ H/C} = 1.12 + 6.74 f_{43} - 17.77 f_{43}^2 \quad (3)$$

$$474 \text{ OSc} = 2 * \text{O/C} - \text{H/C} \quad (4)$$

475 with H/C (and therefore OSc) being estimated only if $f_{44} > 0.05$ and $f_{43} > 0.04$ (Canagaratna et al., 2015).
 476 Uncertainties associated with these estimates - in particular based on ACSM measurements - are
 477 discussed in Sect. S3 (see also Fig. S8). Comparisons with studies using (HR-ToF-) AMS instruments will not
 478 be reported and only variations within this dataset will be discussed (see Sect. S3). Seasonal and annual
 479 O/C, OM/OC, H/C and OSc are shown in Figure 7. High O/C, OM/OC and OSc are found on the annual scale

480 (medians of 0.7, 2.1 and -0.2, respectively), reflecting once more the aged, oxidized properties of organic
481 matter at the study site, consistent with the predominance of the OOA component. Little seasonal
482 variations are observed for the aforementioned variables hence highlighting the high degree of oxidation
483 of OA throughout the year (Figure 7). The unexpectedly high degree of oxygenation of OA observed during
484 cold seasons despite the increased contribution of primary BBOA (with OM/OC ratios of 1.4-1.6) could be
485 explained by the contribution of secondary BBOA in our OOA factor during these cold seasons, which
486 could be associated with the enhancement of e.g. dicarboxylic and ketocarboxylic acid contents (Kundu
487 et al., 2010) that have extremely high OM/OC ratios (up to 3.8 and 3.1, respectively, Turpin and Lim, 2001).
488 This assumption is supported by the higher proportion of f_{60} in our OOA factor (discussed in Sect. 3.2 and
489 S2), as well as the surprisingly high OM/OC ratio observed for OOA during winter (2.5 compared to 2.2-
490 2.4 during the other seasons). Note that Canonaco et al. (2015) also report a higher f_{44} in (LV-) OOA in
491 winter compared to summer in Zurich (Switzerland). According to these authors, this could be due to
492 enhanced aqueous-phase production of (LV-) OOA in clouds or hygroscopic aerosols in winter, which
493 would lead to higher levels of oxygenation compared to gas-phase oxidation mechanisms typically
494 occurring during summer.

495

496 4.3. Possible implications for PM abatement strategies

497 In order to investigate the characteristics of fine aerosol pollution events, the variations of NR-PM₁
498 chemical composition and OA factors' contributions as a function of total NR-PM₁ mass are examined.
499 This investigation is made on the annual (Figure 8, discussion below) and seasonal scales (Fig. S9,
500 discussion in Sect. S4). Distinct trends are observed depending on the chemical species and OA
501 components studied. The proportion of nitrate is clearly enhanced with increasing NR-PM₁ levels (from
502 ~10 to >30% when [NR-PM₁] > 30 µg/m³) indicating that nitrate - or NO_x - abatement policies should be
503 highly effective when attempting to limit PM₁ pollution events in the Upper Po Valley. Sulfate shows an
504 opposite trend with decreasing relative contribution when NR-PM₁ mass increases (e.g. <5% when [NR-
505 PM₁] > 50 µg/m³), likely due to the lower concentrations of sulfate during cold seasons, when the highest
506 number of pollution events is observed. The proportion of organics is substantial (48-66%) independently
507 of NR-PM₁ mass, justifying once again the importance of determining its sources to design adequate
508 abatement policies. When focusing on the organic fraction, BBOA is the only OA factor exhibiting
509 increased contributions (from ~10 to >40%) with increased NR-PM₁ mass (from <10 to >60 µg/m³), which
510 points out the PM abatement potential of effective biomass burning emission reductions. HOA levels are
511 rather constant throughout the year and therefore their proportions steadily decrease when NR-PM₁

512 levels increase, implying that local fossil fuel related emissions of primary OC are not the main responsible
513 for submicron pollution events observed at the study site on the annual scale. Although OOA always
514 represents a major fraction of OA (41-75% depending on the mass bin studied), its contribution steadily
515 decreases with increasing NR-PM₁ mass. This unexpected result signifies that even though aged,
516 secondary, oxidised organics are the main contributor to OA on the annual average (66%), they do not
517 play a prominent role in fine PM acute pollution events.

518 Current European legislations set daily and/or annual PM limit values depending on the size fraction
519 addressed (Directive 2008/50/EC). Volume size distributions suggest that approximately 90% of the PM_{2.5}
520 mass concentration is borne by particles below an aerodynamic diameter of 1 µm at the study site (Putaud
521 et al., 2014a). Therefore, measures tackling the main constituents of the submicron aerosol fraction would
522 be efficient for complying with PM_{2.5} legislations. Based on the chemical characterization of NR-PM₁ and
523 SA of its organic fraction with a time-resolution of 30 min over 1-year, this study provides new evidence
524 which could orient PM abatement strategies also at similar regional background sites of the Po Valley. On
525 the annual scale, OA and especially OOA should be of main concern given their predominance in NR-PM₁
526 chemical composition (Figure 3). On the seasonal scale, efforts should be directed towards the cold
527 seasons (winter and early spring), for which the highest NR-PM₁ levels are observed, due to specific
528 meteorological conditions (e.g. low BLH, low temperatures) and emission sources (e.g. biomass burning,
529 Figure 3 and Figure 5). In particular, measures addressing emissions of NO_x and BBOA would be the most
530 efficient for reducing the magnitude and frequency of PM pollution events (Figure 8).

531 Recommendations for PM abatement strategies are formulated here from a legislative perspective,
532 which aims at decreasing PM levels. Although diminishing PM levels should help reducing PM impacts,
533 the existence of a direct causal relationship can be debatable since each chemical component has a
534 specific effect on human health (WHO, 2013), the radiative forcing (Boucher et al., 2013) or ecosystems
535 (e.g. Carslaw et al., 2010). For instance, implementing policies aiming at mitigating nitrate concentrations
536 - as suggested previously in this section - would likely have limited health benefits according to
537 toxicological studies (Reiss et al., 2007; Schlesinger and Cassee, 2003), and should lead to an increased
538 global warming (Boucher et al., 2013). On the other hand, measures reducing BBOA levels should be
539 beneficial, since the cardio-vascular effects of biomass burning particles have been widely reported in the
540 literature (Bølling et al., 2009; Miljevic et al., 2010; Naeher et al., 2007) and could be similar to those of
541 traffic-emitted particles (WHO, 2013 and references therein), whereas their impacts on the radiative
542 forcing could be null (Boucher et al., 2013). Strategies aiming at reducing solely PM mass are therefore
543 limited, and an assessment of their impacts - e.g. using integrated assessment models (Carnevale et al.,

544 2012; Janssen et al., 2009) with appropriate parameterizations of fundamental processes - would be
545 beneficial.

546

547 5. Conclusion and perspectives

548 The NR-PM₁ chemical composition and the apportionment of the organic fraction have been investigated
549 for the first time with this completeness at a regional background site of the Po valley (Italy), using high
550 time-resolution (30 min) and long term (1 year) measurements with a state-of-the-art quality assured
551 ACSM and the most advanced factor analysis methods. Comparisons between two ACSMs show very good
552 time series correlations for the major compounds ($0.91 < r^2 < 0.98$, $n=1402$) with however discrepancies in
553 their absolute concentrations ($0.9 < \text{slopes} < 1.4$). These results are promising with regard to the consistency
554 of ACSM measurements at different locations, but also underlines the importance of conducting inter-
555 ACSM comparisons to define common protocols and assure data comparability among the European
556 ACSM network (see Crenn et al., 2015). Comparisons between ACSM and independent analytical
557 technique measurements show an overall good agreement for major components throughout the year
558 (typically $r^2 > 0.8$). Discrepancies observed in time series correlations and quantifications (i.e. slopes) for
559 specific species and seasons (e.g. nitrate in summer) are attributed to filter sampling artefacts. These
560 results are encouraging regarding the potential implementation of ACSMs in air quality networks as a
561 replacement of traditional filter-based techniques, to measure the artefact-free chemical composition of
562 fine aerosols with high time-resolution. Additional comparison studies are nevertheless needed to
563 support our results, and further technical development allowing the refractory carbon fraction to be
564 accounted for is required.

565 NR-PM₁ and PM₁ levels measured in the upper Po Valley (14.2 and 15.3 $\mu\text{g}/\text{m}^3$ on the annual
566 average, respectively) are among the highest reported in Europe, stressing the need for implementing
567 effective PM abatement strategies in this region. On average, the chemical composition of non-refractory
568 submicron aerosol is dominated by organic aerosol (58% of NR-PM₁), which is composed of HOA (11% of
569 OA), BBOA (23%) and OOA (66%). Fossil fuel combustion is thus not a major source of primary OA in this
570 area of the Po Valley. Primary BBOA significantly contributes to OA on the annual average and especially
571 during winter (36%). Our OOA component is highly oxidised and aged with an LV-OOA spectral signature,
572 a large proportion of acid-related species and high OM/OC ratios. Highly oxidised OA properties are
573 observed during all seasons, surprisingly including winter, which could reflect secondary BBOA influence
574 and OOA aqueous-phase formation processes during cold seasons. Further research aiming at identifying
575 the sources of OOA - including secondary BBOA using e.g. high resolution mass spectrometric techniques

576 (Crippa et al., 2013) or proton nuclear magnetic resonance (Paglione et al., 2014) - and better estimating
577 O/C, OM/OC and OSc parameters would be beneficial.

578 Specific recommendations for PM abatement strategies at a regional level can be suggested. The
579 higher frequency of particulate pollution peaks observed during cold seasons suggests an orientation of
580 future policies towards these periods. BBOA and nitrate present increasing relative contributions with
581 increasing fine aerosol levels, which suggests that wood burning and NO_x emission reductions should
582 notably decrease NR-PM₁ pollution events. Note that these recommendations are only formulated in the
583 perspective of reducing PM levels, assuming a subsequent reduction of PM impacts. Additional
584 dimensions - e.g. specific impacts of each chemical component, short versus long-term exposure, co-
585 benefit of sanitary and climatic impacts - should also be considered when defining PM abatement
586 strategies. In a broader context, the use of high time resolution analytical techniques for the measurement
587 of PM pollution properties can help better shape our future air quality policies.

588
589 *Acknowledgements.* This study was partially supported by the European Union's project ACTRIS (Aerosols,
590 Clouds, and Trace gases Research InfraStructure Network, EU FP7-262254). R. Passarella (EC-JRC), K.
591 Douglas (EC-JRC), V. Pedroni (EC-JRC) and M. Stracquadanio (ENEA) are thanked for their help on the field
592 and/or for the chemical analyses of filters. P. Croteau (Aerodyne) is acknowledged for his technical
593 support on the operation of the ACSM. N. Jensen (EC-JRC) is thanked for providing gas phase data. M.
594 Crippa (EC-JRC) is acknowledged for her valuable advices.

595 **References**

596

- 597 Aerodyne: Aerosol Chemical Speciation Monitor: Data Acquisition Software Manual, available at:
598 ftp://ftp.aerodyne.com/ACSM/ACSM_Manuals/ACSM_DAQ_Manual.pdf (last access: 15
599 February 2016), 2010a.
- 600 Aerodyne: Aerosol Chemical Speciation Monitor: Data Analysis Software Manual, available at:
601 ftp://ftp.aerodyne.com/ACSM/ACSM_Manuals/ACSM_Igor_Manual.pdf (last access: 15 February
602 2016), 2010b.
- 603 Aiken, A. C., DeCarlo, P. F., Kroll, J. H., Worsnop, D. R., Huffman, J. A., Docherty, K. S., Ulbrich, I. M., Mohr,
604 C., Kimmel, J. R., Sueper, D., Sun, Y., Zhang, Q., Trimborn, A., Northway, M., Ziemann, P. J.,
605 Canagaratna, M. R., Onasch, T. B., Alfarra, M. R., Prevot, A. S. H., Dommen, J., Duplissy, J., Metzger,
606 A., Baltensperger, U., and Jimenez, J. L.: O/C and OM/OC ratios of primary, secondary, and
607 ambient organic aerosols with high-resolution time-of-flight aerosol mass spectrometry, *Environ.*
608 *Sci. Technol.*, 42(12), 4478–4485, doi:10.1021/es703009q, 2008.
- 609 Allan, J. D., Jimenez, J. L., Williams, P. I., Alfarra, M. R., Bower, K. N., Jayne, J. T., Coe, H., and Worsnop, D.
610 R.: Quantitative sampling using an Aerodyne aerosol mass spectrometer 1. Techniques of data
611 interpretation and error analysis, *J. Geophys. Res.-Atmos.*, 108(D3), 4090,
612 doi:10.1029/2002JD002358, 2003a.
- 613 Allan, J. D., Alfarra, M. R., Bower, K. N., Williams, P. I., Gallagher, M. W., Jimenez, J. L., McDonald, A. G.,
614 Nemitz, E., Canagaratna, M. R., Jayne, J. T., Coe, H., and Worsnop, D. R.: Quantitative sampling
615 using an Aerodyne aerosol mass spectrometer 2. Measurements of fine particulate chemical
616 composition in two U.K. cities, *J. Geophys. Res.-Atmos.*, 108(D3), 4091,
617 doi:10.1029/2002JD002359, 2003b.
- 618 Amato, F., Pandolfi, M., Escrig, A., Querol, X., Alastuey, A., Pey, J., Perez, N., and Hopke, P. K.: Quantifying
619 road dust resuspension in urban environment by Multilinear Engine: a comparison with PMF2,
620 *Atmos. Environ.*, 43(17), 2770–2780, doi:10.1016/j.atmosenv.2009.02.039, 2009.
- 621 Belis, C. A., Cancelinha, J., Duane, M., Forcina, V., Pedroni, V., Passarella, R., Tanet, G., Douglas, K.,
622 Piazzalunga, A., Bolzacchini, E., Sangiorgi, G., Perrone, M.-G., Ferrero, L., Fermo, P., and Larsen, B.
623 R.: Sources for PM air pollution in the Po Plain, Italy: I. Critical comparison of methods for
624 estimating biomass burning contributions to benzo(a)pyrene, *Atmos. Environ.*, 45(39), 7266–
625 7275, doi:10.1016/j.atmosenv.2011.08.061, 2011.
- 626 Belis, C. A., Karagulian, F., Larsen, B. R., and Hopke, P. K.: Critical review and meta-analysis of ambient
627 particulate matter source apportionment using receptor models in Europe, *Atmos. Environ.*, 69,
628 94–108, doi:10.1016/j.atmosenv.2012.11.009, 2013.
- 629 Bølling, A. K., Pagels, J., Yttri, K., Barregard, L., Sallsten, G., Schwarze, P. E., and Boman, C.: Health effects
630 of residential wood smoke particles: the importance of combustion conditions and
631 physicochemical particle properties, *Part. Fibre Toxicol.*, 6(1), 29, doi:10.1186/1743-8977-6-29,
632 2009.
- 633 Boucher, O., Randall, D., Artaxo, P., Bretherton, C., Feingold, G., Forster, P., Kerminen, V.-M., Kondo, Y.,
634 Liao, H., Lohmann, U., Rasch, P., Satheesh, S. K., Sherwood, S., Stevens, B., and Zhang, X.: Clouds
635 and aerosols, in *Climate Change 2013: The Physical Science Basis. Contribution of Working Group*
636 *I to the Fifth Assessment Report of the Intergovernmental Panel on Climate Change*, edited by:
637 Stocker, T. F., Qin, D., Plattner, G.-K., Tignor, M., Allen, S. K., Boschung, J., Nauels, A., Xia, Y.,
638 Bex, V., and Midgley, P. M., Cambridge University Press, Cambridge, United Kingdom and New
639 York, NY, USA, 2013.
- 640 Budisulistiorini, S. H., Canagaratna, M. R., Croteau, P. L., Marth, W. J., Baumann, K., Edgerton, E. S., Shaw,
641 S. L., Knipping, E. M., Worsnop, D. R., Jayne, J. T., Gold, A., and Surratt, J. D.: Real-time continuous

642 characterization of secondary organic aerosol derived from isoprene epoxydiols in downtown
643 Atlanta, Georgia, using the Aerodyne aerosol chemical speciation monitor, *Environ. Sci. Technol.*,
644 47(11), 5686–5694, doi:10.1021/es400023n, 2013.

645 Budisulistiorini, S. H., Canagaratna, M. R., Croteau, P. L., Baumann, K., Edgerton, E. S., Kollman, M. S., Ng,
646 N. L., Verma, V., Shaw, S. L., Knipping, E. M., Worsnop, D. R., Jayne, J. T., Weber, R. J., and Surratt,
647 J. D.: Intercomparison of an aerosol chemical speciation monitor (ACSM) with ambient fine
648 aerosol measurements in downtown Atlanta, Georgia, *Atmos. Meas. Tech.*, 7(7), 1929–1941,
649 doi:10.5194/amt-7-1929-2014, 2014.

650 Canagaratna, M. R., Jayne, J. T., Jimenez, J. L., Allan, J. D., Alfarra, M. R., Zhang, Q., Onasch, T. B., Drewnick,
651 F., Coe, H., Middlebrook, A., Delia, A., Williams, L. R., Trimborn, A. M., Northway, M. J., DeCarlo,
652 P. F., Kolb, C. E., Davidovits, P., and Worsnop, D. R.: Chemical and microphysical characterization
653 of ambient aerosols with the Aerodyne aerosol mass spectrometer, *Mass Spectrom. Rev.*, 26(2),
654 185–222, doi:10.1002/mas.20115, 2007.

655 Canagaratna, M. R., Jimenez, J. L., Kroll, J. H., Chen, Q., Kessler, S. H., Massoli, P., Hildebrandt Ruiz, L.,
656 Fortner, E., Williams, L. R., Wilson, K. R., Surratt, J. D., Donahue, N. M., Jayne, J. T., and Worsnop,
657 D. R.: Elemental ratio measurements of organic compounds using aerosol mass spectrometry:
658 characterization, improved calibration, and implications, *Atmos. Chem. Phys.*, 15, 253–272,
659 doi:10.5194/acp-15-253-2015, 2015.

660 Canonaco, F., Crippa, M., Slowik, J. G., Baltensperger, U., and Prévôt, A. S. H.: SoFi, an IGOR-based interface
661 for the efficient use of the generalized multilinear engine (ME-2) for the source apportionment:
662 ME-2 application to aerosol mass spectrometer data, *Atmos. Meas. Tech.*, 6(12), 3649–3661,
663 doi:10.5194/amt-6-3649-2013, 2013.

664 Canonaco, F., Slowik, J. G., Baltensperger, U., and Prévôt, A. S. H.: Seasonal differences in oxygenated
665 organic aerosol composition: implications for emissions sources and factor analysis, *Atmos. Chem.*
666 *Phys.*, 15(12), 6993–7002, doi:10.5194/acp-15-6993-2015, 2015.

667 Carbone, C., Decesari, S., Paglione, M., Giulianelli, L., Rinaldi, M., Marinoni, A., Cristofanelli, P., Diodato,
668 A., Bonasoni, P., Fuzzi, S., and Facchini, M. C.: 3-year chemical composition of free tropospheric
669 PM₁ at the Mt. Cimone GAW global station – South Europe – 2165 m a.s.l., *Atmos. Environ.*, 87,
670 218–227, doi:10.1016/j.atmosenv.2014.01.048, 2014.

671 Carnevale, C., Finzi, G., Pisoni, E., Volta, M., Guariso, G., Gianfreda, R., Maffei, G., Thunis, P., White, L.,
672 and Triacchini, G.: An integrated assessment tool to define effective air quality policies at regional
673 scale, *Environ. Modell. Softw.*, 38, 306–315, doi:10.1016/j.envsoft.2012.07.004, 2012.

674 Carslaw, K. S., Boucher, O., Spracklen, D. V., Mann, G. W., Rae, J. G. L., Woodward, S., and Kulmala, M.: A
675 review of natural aerosol interactions and feedbacks within the Earth system, *Atmos. Chem. Phys.*,
676 10(4), 1701–1737, 2010.

677 Cavalli, F., Viana, M., Yttri, K. E., Genberg, J., and Putaud, J. P.: Toward a standardised thermal-optical
678 protocol for measuring atmospheric organic and elemental carbon: the EUSAAR protocol, *Atmos.*
679 *Meas. Tech.*, 3, 79–89, 2010.

680 Chow, J. C., Watson, J. G., Lowenthal, D. H., and Magliano, K. L.: Loss of PM_{2.5} nitrate from filter samples
681 in central California, *J. Air Waste Manage. Assoc.*, 55(8), 1158–1168,
682 doi:10.1080/10473289.2005.10464704, 2005.

683 Clegg, S. L., Brimblecombe, P., and Wexler, A. S.: Thermodynamic model of the system H⁺-NH₄⁺-SO₄²⁻
684 -NO₃⁻-H₂O at tropospheric temperatures, *J. Phys. Chem. A*, 102(12), 2137–2154,
685 doi:10.1021/jp973042r, 1998.

686 Clerici, M. and Mélin, F.: Aerosol direct radiative effect in the Po Valley region derived from AERONET
687 measurements, *Atmos. Chem. Phys.*, 8(16), 4925–4946, 2008.

688 Crawford, J., Cohen, D., Dyer, L., and Zahorowski, W.: Receptor modelling with PMF2 and ME2 using
689 aerosol data from Hong Kong, Australian Nuclear Science and Technology Organisation (ANSTO),

690 available at: <http://apo.ansto.gov.au/dspace/bitstream/10238/201/1/ANSTO-E-756.pdf> (last
691 access: 15 February 2016), 2005.

692 Crenn, V., Sciare, J., Croteau, P. L., Verlhac, S., Fröhlich, R., Belis, C. A., Aas, W., Äijälä, M., Alastuey, A.,
693 Artiñano, B., Baisnée, D., Bonnaire, N., Bressi, M., Canagaratna, M., Canonaco, F., Carbone, C.,
694 Cavalli, F., Coz, E., Cubison, M. J., Esser-Gietl, J. K., Green, D. C., Gros, V., Heikkinen, L., Herrmann,
695 H., Lunder, C., Minguillón, M. C., Močnik, G., O'Dowd, C. D., Ovadnevaite, J., Petit, J.-E., Petralia,
696 E., Poulain, L., Priestman, M., Riffault, V., Ripoll, A., Sarda-Estève, R., Slowik, J. G., Setyan, A.,
697 Wiedensohler, A., Baltensperger, U., Prévôt, A. S. H., Jayne, J. T., and Favez, O.: ACTRIS ACSM
698 intercomparison – part 1: reproducibility of concentration and fragment results from 13 individual
699 quadrupole aerosol chemical speciation monitors (Q-ACSM) and consistency with co-located
700 instruments, *Atmos. Meas. Tech.*, 8(12), 5063–5087, doi:10.5194/amt-8-5063-2015, 2015.

701 Crippa, M., DeCarlo, P. F., Slowik, J. G., Mohr, C., Heringa, M. F., Chirico, R., Poulain, L., Freutel, F., Sciare,
702 J., Cozic, J., Di Marco, C. F., Elsasser, M., Nicolas, J. B., Marchand, N., Abidi, E., Wiedensohler, A.,
703 Drewnick, F., Schneider, J., Borrmann, S., Nemitz, E., Zimmermann, R., Jaffrezo, J.-L., Prévôt, A. S.
704 H., and Baltensperger, U.: Wintertime aerosol chemical composition and source apportionment
705 of the organic fraction in the metropolitan area of Paris, *Atmos. Chem. Phys.*, 13(2), 961–981,
706 doi:10.5194/acp-13-961-2013, 2013.

707 Crippa, M., Canonaco, F., Lanz, V. A., Äijälä, M., Allan, J. D., Carbone, S., Capes, G., Ceburnis, D., Dall'Osto,
708 M., Day, D. A., DeCarlo, P. F., Ehn, M., Eriksson, A., Freney, E., Hildebrandt Ruiz, L., Hillamo, R.,
709 Jimenez, J. L., Junninen, H., Kiendler-Scharr, A., Kortelainen, A.-M., Kulmala, M., Laaksonen, A.,
710 Mensah, A. A., Mohr, C., Nemitz, E., O'Dowd, C., Ovadnevaite, J., Pandis, S. N., Petäjä, T., Poulain,
711 L., Saarikoski, S., Sellegri, K., Swietlicki, E., Tiitta, P., Worsnop, D. R., Baltensperger, U., and Prévôt,
712 A. S. H.: Organic aerosol components derived from 25 AMS data sets across Europe using a
713 consistent ME-2 based source apportionment approach, *Atmos. Chem. Phys.*, 14(12), 6159–6176,
714 doi:10.5194/acp-14-6159-2014, 2014.

715 Cubison, M. J., Ortega, A. M., Hayes, P. L., Farmer, D. K., Day, D., Lechner, M. J., Brune, W. H., Apel, E.,
716 Diskin, G. S., Fisher, J. A., Fuelberg, H. E., Hecobian, A., Knapp, D. J., Mikoviny, T., Riemer, D.,
717 Sachse, G. W., Sessions, W., Weber, R. J., Weinheimer, A. J., Wisthaler, A., and Jimenez, J. L.:
718 Effects of aging on organic aerosol from open biomass burning smoke in aircraft and laboratory
719 studies, *Atmos. Chem. Phys.*, 11(23), 12049–12064, doi:10.5194/acp-11-12049-2011, 2011.

720 Dall'Osto, M., Paglione, M., Decesari, S., Facchini, M. C., O'Dowd, C., Plass-Duellmer, C., and Harrison, R.
721 M.: On the Origin of AMS “Cooking Organic Aerosol” at a Rural Site, *Environ. Sci. Technol.*, 49(24),
722 13964–13972, doi:10.1021/acs.est.5b02922, 2015.

723 Daumit, K. E., Kessler, S. H., and Kroll, J. H.: Average chemical properties and potential formation pathways
724 of highly oxidized organic aerosol, *Faraday Discuss.*, 165, 181, doi:10.1039/c3fd00045a, 2013.

725 Decesari, S., Allan, J., Plass-Duellmer, C., Williams, B. J., Paglione, M., Facchini, M. C., O'Dowd, C.,
726 Harrison, R. M., Gietl, J. K., Coe, H., Giulianelli, L., Gobbi, G. P., Lanconelli, C., Carbone, C.,
727 Worsnop, D., Lambe, A. T., Ahern, A. T., Moretti, F., Tagliavini, E., Elste, T., Gilge, S., Zhang, Y., and
728 Dall'Osto, M.: Measurements of the aerosol chemical composition and mixing state in the Po
729 Valley using multiple spectroscopic techniques, *Atmos. Chem. Phys.*, 14, 12109–12132,
730 doi:10.5194/acp-14-12109-2014, 2014.

731 Duplissy, J., DeCarlo, P. F., Dommen, J., Alfarra, M. R., Metzger, A., Barmapadimos, I., Prevot, A. S. H.,
732 Weingartner, E., Tritscher, T., Gysel, M., Aiken, A. C., Jimenez, J. L., Canagaratna, M. R., Worsnop,
733 D. R., Collins, D. R., Tomlinson, J., and Baltensperger, U.: Relating hygroscopicity and composition
734 of organic aerosol particulate matter, *Atmos. Chem. Phys.*, 11(3), 1155–1165, doi:10.5194/acp-
735 11-1155-2011, 2011.

736 EC: Commission of the European communities, Commission staff working paper, Annex to the
737 communication on thematic strategy on air pollution and the directive on “Ambient air quality

738 and cleaner air for Europe”, Impact assessment, SEC (2005) 1133, available at:
739 http://ec.europa.eu/environment/archives/cafe/pdf/ia_report_en050921_final.pdf (last access:
740 15 February 2016), 2005.

741 EEA: Air quality in Europe - 2013 report, European Environment Agency (EEA), report no 9/2013,
742 publication, available at: <http://www.eea.europa.eu/publications/air-quality-in-europe-2013>
743 (last access: 15 February 2016), 2013.

744 Ervens, B., Turpin, B. J., and Weber, R. J.: Secondary organic aerosol formation in cloud droplets and
745 aqueous particles (aqSOA): a review of laboratory, field and model studies, *Atmos. Chem. Phys.*,
746 11(21), 11069–11102, doi:10.5194/acp-11-11069-2011, 2011.

747 EU: Directive 2008/50/EC of the European Parliament and of the Council of 21 May 2008 on ambient air
748 quality and cleaner air for Europe, available at [http://eur-lex.europa.eu/legal-](http://eur-lex.europa.eu/legal-content/en/ALL/?uri=CELEX:32008L0050)
749 [content/en/ALL/?uri=CELEX:32008L0050](http://eur-lex.europa.eu/legal-content/en/ALL/?uri=CELEX:32008L0050) (last access 18 July 2016), 2008.

750 Ferrero, L., Castelli, M., Ferrini, B. S., Moscatelli, M., Perrone, M. G., Sangiorgi, G., D’Angelo, L., Rovelli, G.,
751 Moroni, B., Scardazza, F., Močnik, G., Bolzacchini, E., Petitta, M., and Cappelletti, D.: Impact of
752 black carbon aerosol over Italian basin valleys: high-resolution measurements along vertical
753 profiles, radiative forcing and heating rate, *Atmos. Chem. Phys.*, 14(18), 9641–9664,
754 doi:10.5194/acp-14-9641-2014, 2014.

755 Fröhlich, R., Crenn, V., Setyan, A., Belis, C. A., Canonaco, F., Favez, O., Riffault, V., Slowik, J. G., Aas, W.,
756 Aijälä, M., Alastuey, A., Artiñano, B., Bonnaire, N., Bozzetti, C., Bressi, M., Carbone, C., Coz, E.,
757 Croteau, P. L., Cubison, M. J., Esser-Gietl, J. K., Green, D. C., Gros, V., Heikkinen, L., Herrmann, H.,
758 Jayne, J. T., Lunder, C. R., Minguillón, M. C., Močnik, G., O’Dowd, C. D., Ovadnevaite, J., Petralia,
759 E., Poulain, L., Priestman, M., Ripoll, A., Sarda-Estève, R., Wiedensohler, A., Baltensperger, U.,
760 Sciare, J., and Prévôt, A. S. H.: ACTRIS ACSM intercomparison – part 2: intercomparison of ME-2
761 organic source apportionment results from 15 individual, co-located aerosol mass spectrometers,
762 *Atmos. Meas. Tech.*, 8(6), 2555–2576, doi:10.5194/amt-8-2555-2015, 2015.

763 Gaeggeler, K., Prevot, A. S. H., Dommen, J., Legreid, G., Reimann, S., and Baltensperger, U.: Residential
764 wood burning in an Alpine valley as a source for oxygenated volatile organic compounds,
765 hydrocarbons and organic acids, *Atmos. Environ.*, 42(35), 8278–8287,
766 doi:10.1016/j.atmosenv.2008.07.038, 2008.

767 Gentner, D. R., Isaacman, G., Worton, D. R., Chan, A. W. H., Dallmann, T. R., Davis, L., Liu, S., Day, D. A.,
768 Russell, L. M., Wilson, K. R., Weber, R., Guha, A., Harley, R. A., and Goldstein, A. H.: Elucidating
769 secondary organic aerosol from diesel and gasoline vehicles through detailed characterization of
770 organic carbon emissions, *Proc. Natl. Acad. Sci. USA*, 109(45), 18318–18323,
771 doi:10.1073/pnas.1212272109, 2012.

772 Gilardoni, S., Vignati, E., Cavalli, F., Putaud, J. P., Larsen, B. R., Karl, M., Stenström, K., Genberg, J., Henne,
773 S., and Dentener, F.: Better constraints on sources of carbonaceous aerosols using a combined ¹⁴C
774 – macro tracer analysis in a European rural background site, *Atmos. Chem. Phys.*, 11(12), 5685–
775 5700, doi:10.5194/acp-11-5685-2011, 2011.

776 Gilardoni, S., Massoli, P., Giulianelli, L., Rinaldi, M., Paglione, M., Pollini, F., Lanconelli, C., Poluzzi, V.,
777 Carbone, S., Hillamo, R., Russell, L. M., Facchini, M. C., and Fuzzi, S.: Fog scavenging of organic and
778 inorganic aerosol in the Po Valley, *Atmos. Chem. Phys.*, 14(13), 6967–6981, doi:10.5194/acp-14-
779 6967-2014, 2014.

780 Hand, J. L. and Kreidenweis, S. M.: A new method for retrieving particle refractive index and effective
781 density from aerosol size distribution data, *Aerosol Sci. Tech.*, 36(10), 1012–1026,
782 doi:10.1080/02786820290092276, 2002.

783 Herich, H., Gianini, M. F. D., Piot, C., Močnik, G., Jaffrezo, J.-L., Besombes, J.-L., Prévôt, A. S. H., and Hueglin,
784 C.: Overview of the impact of wood burning emissions on carbonaceous aerosols and PM in large

785 parts of the Alpine region, *Atmos. Environ.*, 49, 64–75, doi:10.1016/j.atmosenv.2014.02.008,
786 2014.

787 Heringa, M. F., DeCarlo, P. F., Chirico, R., Tritscher, T., Dommen, J., Weingartner, E., Richter, R., Wehrle,
788 G., Prévôt, A. S. H., and Baltensperger, U.: Investigations of primary and secondary particulate
789 matter of different wood combustion appliances with a high-resolution time-of-flight aerosol
790 mass spectrometer, *Atmos. Chem. Phys.*, 11(12), 5945–5957, doi:10.5194/acp-11-5945-2011,
791 2011.

792 Hu, M., Peng, J., Sun, K., Yue, D., Guo, S., Wiedensohler, A., and Wu, Z.: Estimation of size-resolved ambient
793 particle density based on the measurement of aerosol number, mass, and chemical size
794 distributions in the winter in Beijing, *Environ. Sci. Technol.*, 46(12), 120830075118007,
795 doi:10.1021/es204073t, 2012.

796 Huang, X.-F., He, L.-Y., Hu, M., Canagaratna, M. R., Sun, Y., Zhang, Q., Zhu, T., Xue, L., Zeng, L.-W., Liu, X.-
797 G., Zhang, Y.-H., Jayne, J. T., Ng, N. L., and Worsnop, D. R.: Highly time-resolved chemical
798 characterization of atmospheric submicron particles during 2008 Beijing Olympic Games using an
799 aerodyne high-resolution aerosol mass spectrometer, *Atmos. Chem. Phys.*, 10(18), 8933–8945,
800 doi:10.5194/acp-10-8933-2010, 2010.

801 Janssen, S., Ewert, F., Li, H., Athanasiadis, I. N., Wien, J. J. F., Thérond, O., Knapen, M. J. R., Bezlepikina, I.,
802 Alkan-Olsson, J., Rizzoli, A. E., Belhouchette, H., Svensson, M., and van Ittersum, M. K.: Defining
803 assessment projects and scenarios for policy support: use of ontology in integrated assessment
804 and modelling, *Environ. Modell. Softw.*, 24(12), 1491–1500, doi:10.1016/j.envsoft.2009.04.009,
805 2009.

806 Jayne, J. T., Leard, D. C., Zhang, X., Davidovits, P., Smith, K. A., Kolb, C. E., and Worsnop, D. R.: Development
807 of an aerosol mass spectrometer for size and composition analysis of submicron particles, *Aerosol
808 Sci. Tech.*, 33(1-2), 49–70, 2000.

809 Jimenez, J. L., Canagaratna, M. R., Donahue, N. M., Prevot, A. S. H., Zhang, Q., Kroll, J. H., DeCarlo, P. F.,
810 Allan, J. D., Coe, H., Ng, N. L., Aiken, A. C., Docherty, K. S., Ulbrich, I. M., Grieshop, A. P., Robinson,
811 A. L., Duplissy, J., Smith, J. D., Wilson, K. R., Lanz, V. A., Hueglin, C., Sun, Y. L., Tian, J., Laaksonen,
812 A., Raatikainen, T., Rautiainen, J., Vaattovaara, P., Ehn, M., Kulmala, M., Tomlinson, J. M., Collins,
813 D. R., Cubison, M. J., Dunlea, J., Huffman, J. A., Onasch, T. B., Alfarra, M. R., Williams, P. I., Bower,
814 K., Kondo, Y., Schneider, J., Drewnick, F., Borrmann, S., Weimer, S., Demerjian, K., Salcedo, D.,
815 Cottrell, L., Griffin, R., Takami, A., Miyoshi, T., Hatakeyama, S., Shimono, A., Sun, J. Y., Zhang, Y.
816 M., Dzepina, K., Kimmel, J. R., Sueper, D., Jayne, J. T., Herndon, S. C., Trimborn, A. M., Williams, L.
817 R., Wood, E. C., Middlebrook, A. M., Kolb, C. E., Baltensperger, U., and Worsnop, D. R.: Evolution
818 of organic aerosols in the atmosphere, *Science*, 326(5959), 1525–1529,
819 doi:10.1126/science.1180353, 2009.

820 Kroll, J. H., Donahue, N. M., Jimenez, J. L., Kessler, S. H., Canagaratna, M. R., Wilson, K. R., Altieri, K. E.,
821 Mazzoleni, L. R., Wozniak, A. S., Bluhm, H., Mysak, E. R., Smith, J. D., Kolb, C. E., and Worsnop, D.
822 R.: Carbon oxidation state as a metric for describing the chemistry of atmospheric organic aerosol,
823 *Nat. Chem.*, 3(2), 133–139, doi:10.1038/nchem.948, 2011.

824 Kukkonen, J., Pohjola, M., Ssokhi, R., Luhana, L., Kitwiroon, N., Fragkou, L., Rantamaki, M., Berge, E.,
825 Odegaard, V., and Havardslordal, L.: Analysis and evaluation of selected local-scale PM air
826 pollution episodes in four European cities: Helsinki, London, Milan and Oslo, *Atmos. Environ.*,
827 39(15), 2759–2773, doi:10.1016/j.atmosenv.2004.09.090, 2005.

828 Kundu, S., Kawamura, K., Andreae, T. W., Hoffer, A., and Andreae, M. O.: Molecular distributions of
829 dicarboxylic acids, ketocarboxylic acids and α -dicarbonyls in biomass burning aerosols:
830 implications for photochemical production and degradation in smoke layers, *Atmos. Chem. Phys.*,
831 10(5), 2209–2225, doi:10.5194/acp-10-2209-2010, 2010.

832 Lanz, V. A., Alfarra, M. R., Baltensperger, U., Buchmann, B., Hueglin, C., and Prévôt, A. S. H.: Source
833 apportionment of submicron organic aerosols at an urban site by factor analytical modelling of
834 aerosol mass spectra, *Atmos. Chem. Phys.*, 7(6), 1503–1522, doi:10.5194/acp-7-1503-2007, 2007.

835 Lanz, V. A., Prévôt, A. S. H., Alfarra, M. R., Weimer, S., Mohr, C., DeCarlo, P. F., Gianini, M. F. D., Hueglin,
836 C., Schneider, J., Favez, O., D’Anna, B., George, C., and Baltensperger, U.: Characterization of
837 aerosol chemical composition with aerosol mass spectrometry in Central Europe: an overview,
838 *Atmos. Chem. Phys.*, 10(21), 10453–10471, 2010.

839 Larsen, B. R., Gilardoni, S., Stenström, K., Niedzialek, J., Jimenez, J., and Belis, C. A.: Sources for PM air
840 pollution in the Po Plain, Italy: II. Probabilistic uncertainty characterization and sensitivity analysis
841 of secondary and primary sources, *Atmos. Environ.*, 50, 203–213,
842 doi:10.1016/j.atmosenv.2011.12.038, 2012.

843 Larssen, S., Sluyter, R., and Helmis, C.: Criteria for EUROAIRNET, the EEA Air Quality Monitoring and
844 Information Network, available at:
845 http://www.eea.europa.eu/publications/TEC12/at_download/file (last access: 10 February
846 2016), 1999.

847 Lee, T., Sullivan, A. P., Mack, L., Jimenez, J. L., Kreidenweis, S. M., Onasch, T. B., Worsnop, D. R., Malm, W.,
848 Wold, C. E., Hao, W. M., and Collett, J. L.: Chemical smoke marker emissions during flaming and
849 smoldering phases of laboratory open burning of wildland fuels, *Aerosol Sci. Tech.*, 44(9), i–v,
850 doi:10.1080/02786826.2010.499884, 2010.

851 Liu, P. S. K., Deng, R., Smith, K. A., Williams, L. R., Jayne, J. T., Canagaratna, M. R., Moore, K., Onasch, T. B.,
852 Worsnop, D. R., and Deshler, T.: Transmission efficiency of an aerodynamic focusing lens system:
853 comparison of model calculations and laboratory measurements for the Aerodyne aerosol mass
854 spectrometer, *Aerosol Sci. Tech.*, 41(8), 721–733, doi:10.1080/02786820701422278, 2007.

855 Maimone, F., Turpin, B. J., Solomon, P., Meng, Q., Robinson, A. L., Subramanian, R., and Polidori, A.:
856 Correction methods for organic carbon artifacts when using quartz-fiber filters in large particulate
857 matter monitoring networks: the regression method and other options, *J. Air Waste Manage.*
858 *Assoc.*, 61(6), 696–710, doi:10.3155/1047-3289.61.6.696, 2011.

859 McMurry, P. H., Wang, X., Park, K., and Ehara, K.: The relationship between mass and mobility for
860 atmospheric particles: a new technique for measuring particle density, *Aerosol Sci. Tech.*, 36(2),
861 227–238, doi:10.1080/027868202753504083, 2002.

862 Middlebrook, A. M., Bahreini, R., Jimenez, J. L., and Canagaratna, M. R.: Evaluation of composition-
863 dependent collection efficiencies for the Aerodyne aerosol mass spectrometer using field data,
864 *Aerosol Sci. Tech.*, 46(3), 258–271, doi:10.1080/02786826.2011.620041, 2012.

865 Miljevic, B., Heringa, M. F., Keller, A., Meyer, N. K., Good, J., Lauber, A., Decarlo, P. F., Fairfull-Smith, K. E.,
866 Nussbaumer, T., Burtscher, H., Prévôt, A. S. H., Baltensperger, U., Bottle, S. E., and Ristovski, Z. D.:
867 Oxidative potential of logwood and pellet burning particles assessed by a novel profluorescent
868 nitroxide probe, *Environ. Sci. Technol.*, 44(17), 6601–6607, 2010.

869 Minguillón, M. C., Ripoll, A., Pérez, N., Prévôt, A. S. H., Canonaco, F., Querol, X., and Alastuey, A.: Chemical
870 characterization of submicron regional background aerosols in the western Mediterranean using
871 an aerosol chemical speciation monitor, *Atmos. Chem. Phys.*, 15(11), 6379–6391,
872 doi:10.5194/acp-15-6379-2015, 2015.

873 Naeher, L. P., Brauer, M., Lipsett, M., Zelikoff, J. T., Simpson, C. D., Koenig, J. Q., and Smith, K. R.:
874 Woodsmoke health effects: a review, *Inhal. Toxicol.*, 19(1), 67–106,
875 doi:10.1080/08958370600985875, 2007.

876 Ng, N. L., Herndon, S. C., Trimborn, A., Canagaratna, M. R., Croteau, P. L., Onasch, T. B., Sueper, D.,
877 Worsnop, D. R., Zhang, Q., Sun, Y. L., and Jayne, J. T.: An aerosol chemical speciation monitor
878 (ACSM) for routine monitoring of the composition and mass concentrations of ambient aerosol,
879 *Aerosol Sci. Tech.*, 45(7), 780–794, doi:10.1080/02786826.2011.560211, 2011a.

880 Ng, N. L., Canagaratna, M. R., Jimenez, J. L., Chhabra, P. S., Seinfeld, J. H., and Worsnop, D. R.: Changes in
881 organic aerosol composition with aging inferred from aerosol mass spectra, *Atmos. Chem. Phys.*,
882 11(13), 6465–6474, doi:10.5194/acp-11-6465-2011, 2011b.

883 Ng, N. L., Canagaratna, M. R., Jimenez, J. L., Zhang, Q., Ulbrich, I. M., and Worsnop, D. R.: Real-time
884 methods for estimating organic component mass concentrations from aerosol mass spectrometer
885 data, *Environ. Sci. Technol.*, 45(3), 910–916, doi:10.1021/es102951k, 2011c.

886 Paatero, P.: User's guide for the multilinear engine program "ME2" for fitting multilinear and
887 quasimultilinear models, University of Helsinki, Finland, 2000.

888 Paatero, P. and Tapper, U.: Positive matrix factorization - a nonnegative factor model with optimal
889 utilization of error-estimates of data values, *Environmetrics*, 5(2), 111–126,
890 doi:10.1002/env.3170050203, 1994.

891 Paglione, M., Saarikoski, S., Carbone, S., Hillamo, R., Facchini, M. C., Finessi, E., Giulianelli, L., Carbone, C.,
892 Fuzzi, S., Moretti, F., Tagliavini, E., Swietlicki, E., Eriksson Stenström, K., Prévôt, A. S. H., Massoli,
893 P., Canaragatna, M., Worsnop, D., and Decesari, S.: Primary and secondary biomass burning
894 aerosols determined by proton nuclear magnetic resonance (¹H-NMR) spectroscopy during the
895 2008 EUCAARI campaign in the Po Valley (Italy), *Atmos. Chem. Phys.*, 14(10), 5089–5110,
896 doi:10.5194/acp-14-5089-2014, 2014.

897 Pernigotti, D., Georgieva, E., Thunis, P., and Bessagnet, B.: Impact of meteorology on air quality modeling
898 over the Po valley in northern Italy, *Atmos. Environ.*, 51, 303–310,
899 doi:10.1016/j.atmosenv.2011.12.059, 2012.

900 Perrone, M. G., Larsen, B. R., Ferrero, L., Sangiorgi, G., De Gennaro, G., Udisti, R., Zangrando, R., Gambaro,
901 A., and Bolzacchini, E.: Sources of high PM_{2.5} concentrations in Milan, northern Italy: molecular
902 marker data and CMB modelling, *Sci. Total Environ.*, 414, 343–355,
903 doi:10.1016/j.scitotenv.2011.11.026, 2012.

904 Petit, J.-E., Favez, O., Sciare, J., Crenn, V., Sarda-Estève, R., Bonnaire, N., Močnik, G., Dupont, J.-C.,
905 Haeffelin, M., and Leoz-Garziandia, E.: Two years of near real-time chemical composition of
906 submicron aerosols in the region of Paris using an aerosol chemical speciation monitor (ACSM)
907 and a multi-wavelength aethalometer, *Atmos. Chem. Phys.*, 15, 2985–3005, doi:10.5194/acp-15-
908 2985-2015, 2015.

909 Pitz, M., Cyrys, J., Karg, E., Wiedensohler, A., Wichmann, H.-E., and Heinrich, J.: Variability of apparent
910 particle density of an urban aerosol, *Environ. Sci. Technol.*, 37(19), 4336–4342,
911 doi:10.1021/es034322p, 2003.

912 Pitz, M., Schmid, O., Heinrich, J., Birmili, W., Maguhn, J., Zimmermann, R., Wichmann, H.-E., Peters, A.,
913 and Cyrys, J.: Seasonal and diurnal variation of PM_{2.5} apparent particle density in urban air in
914 Augsburg, Germany, *Environ. Sci. Technol.*, 42(14), 5087–5093, 2008.

915 Putaud, J. P., Van Dingenen, R., and Raes, F.: Submicron aerosol mass balance at urban and semirural sites
916 in the Milan area (Italy), *J. Geophys. Res.-Atmos.*, 107(D22), LOP 11–1–LOP 11–10,
917 doi:10.1029/2000JD000111, 2002.

918 Putaud, J.-P., Van Dingenen, R., Alastuey, A., Bauer, H., Birmili, W., Cyrys, J., Flentje, H., Fuzzi, S., Gehrig,
919 R., Hansson, H. C., Harrison, R. M., Herrmann, H., Hitzenberger, R., Hüglin, C., Jones, A. M., Kasper-
920 Giebl, A., Kiss, G., Kousa, A., Kuhlbusch, T. A. J., Loschau, G., Maenhaut, W., Molnar, A., Moreno,
921 T., Pekkanen, J., Perrino, C., Pitz, M., Puxbaum, H., Querol, X., Rodriguez, S., Salma, I., Schwarz, J.,
922 Smolik, J., Schneider, J., Spindler, G., ten Brink, H., Tursic, J., Viana, M., Wiedensohler, A., and
923 Raes, F.: A European aerosol phenomenology – 3: physical and chemical characteristics of
924 particulate matter from 60 rural, urban, and kerbside sites across Europe, *Atmos. Environ.*, 44,
925 1308–1320, 2010.

926 Putaud, J.-P., Adam, M., Belis, C. A., Bergamaschi, P., Cancellinha, J., Cavalli, F., Cescatti, A., Daou, D.,
927 Dell'Acqua, A., Douglas, K., Duerr, M., Goded, I., Grassi, F., Gruening, C., Hjorth, J., Jensen, N. R.,

928 Lagler, F., Manca, G., Martins Dos Santos, S., Passarella, R., Pedroni, V., Rocha e Abreu, P., Roux,
929 D., Scheeren, B., and Schembari, C.: JRC-Ispra Atmosphere-Biosphere-Climate Integrated
930 monitoring Station (ABC-IS): 2011 report, JRC Technical Reports, Joint Research Centre, Ispra
931 (Italy), available at:
932 [http://publications.jrc.ec.europa.eu/repository/bitstream/111111111/28242/1/lb-na-25753-en-](http://publications.jrc.ec.europa.eu/repository/bitstream/111111111/28242/1/lb-na-25753-en-n.pdf)
933 [n.pdf](http://publications.jrc.ec.europa.eu/repository/bitstream/111111111/28242/1/lb-na-25753-en-n.pdf) (last access: 28 March 2014), 2013.

934 Putaud, J.-P., Bergamaschi, P., Bressi, M., Cavalli, F., Cescatti, A., Daou, D., Dell'acqua, A., Douglas, K.,
935 Duerr, M., Fumagalli, I., Goded Ballarin, I., Grassi, F., Gruening, C., Hjorth, J., Jensen, N., Lagler, F.,
936 Manca, G., Martins Dos Santos, S., Matteucci, M., Passarella, R., Pedroni, V., Pokorska, O., and
937 Roux, D.: JRC – Ispra Atmosphere – Biosphere – Climate Integrated monitoring Station 2013
938 report, EUR - Scientific and Technical Research Reports, Publications Office of the European
939 Union, available at: <http://publications.jrc.ec.europa.eu/repository/handle/111111111/33904>
940 (last access: 19 February 2015), 2014a.

941 Putaud, J. P., Cavalli, F., Martins dos Santos, S., and Dell'Acqua, A.: Long-term trends in aerosol optical
942 characteristics in the Po Valley, Italy, *Atmos. Chem. Phys.*, 14(17), 9129–9136, doi:10.5194/acp-
943 14-9129-2014, 2014b.

944 Reiss, R., Anderson, E. L., Cross, C. E., Hidy, G., Hoel, D., McClellan, R., and Moolgavkar, S.: Evidence of
945 health impacts of sulfate- and nitrate-containing particles in ambient air, *Inhal. Toxicol.*, 19(5),
946 419–449, doi:10.1080/08958370601174941, 2007.

947 Riffault, V., Zhang, S., Tison, E., and Setyan, A.: Chloride RIE measurements, 14th AMS user meeting, 8
948 September 2013, available at: [http://cires.colorado.edu/jimenez-](http://cires.colorado.edu/jimenez-group/UsrMtg/UsrsMtg14/AMS_user_meeting_ChI_RIE_riffault.pdf)
949 [group/UsrMtg/UsrsMtg14/AMS_user_meeting_ChI_RIE_riffault.pdf](http://cires.colorado.edu/jimenez-group/UsrMtg/UsrsMtg14/AMS_user_meeting_ChI_RIE_riffault.pdf) (last access: 10 February
950 2016), 2013.

951 Ripoll, A., Minguillón, M. C., Pey, J., Jimenez, J. L., Day, D. A., Sosedova, Y., Canonaco, F., Prévôt, A. S. H.,
952 Querol, X., and Alastuey, A.: Long-term real-time chemical characterization of submicron aerosols
953 at Montsec (southern Pyrenees, 1570 m a.s.l.), *Atmos. Chem. Phys.*, 15(6), 2935–2951,
954 doi:10.5194/acp-15-2935-2015, 2015.

955 Saarikoski, S., Carbone, S., Decesari, S., Giulianelli, L., Angelini, F., Canagaratna, M., Ng, N. L., Trimborn, A.,
956 Facchini, M. C., Fuzzi, S., Hillamo, R., and Worsnop, D.: Chemical characterization of springtime
957 submicrometer aerosol in Po Valley, Italy, *Atmos. Chem. Phys.*, 12(18), 8401–8421,
958 doi:10.5194/acp-12-8401-2012, 2012.

959 Schaap, M., Van Loon, M., Ten Brink, H. M., Dentener, F. J., and Bultjes, P. J. H.: Secondary inorganic
960 aerosol simulations for Europe with special attention to nitrate, *Atmos. Chem. Phys.*, 4(3), 857–
961 874, 2004.

962 Schlesinger, R. B. and Cassee, F.: Atmospheric secondary inorganic particulate matter: the toxicological
963 perspective as a basis for health effects risk assessment, *Inhal. Toxicol.*, 15(3), 197–235,
964 doi:10.1080/08958370390168247, 2003.

965 Seinfeld, J. H. and Pandis, S. N.: *Atmospheric Chemistry and Physics: from Air Pollution to Climate Change*,
966 Wiley, New York, USA, 2006.

967 Sturtz, T. M., Adar, S. D., Gould, T., and Larson, T. V.: Constrained source apportionment of coarse
968 particulate matter and selected trace elements in three cities from the multi-ethnic study of
969 atherosclerosis, *Atmos. Environ.*, 44, 65–77, doi:10.1016/j.atmosenv.2013.11.031, 2014.

970 Sun, Y., Wang, Z., Dong, H., Yang, T., Li, J., Pan, X., Chen, P., and Jayne, J. T.: Characterization of summer
971 organic and inorganic aerosols in Beijing, China with an aerosol chemical speciation monitor,
972 *Atmos. Environ.*, 51, 250–259, doi:10.1016/j.atmosenv.2012.01.013, 2012.

973 Takegawa, N., Miyazaki, Y., Kondo, Y., Komazaki, Y., Miyakawa, T., Jimenez, J. L., Jayne, J. T., Worsnop, D.
974 R., Allan, J. D., and Weber, R. J.: Characterization of an Aerodyne aerosol mass spectrometer

975 (AMS): intercomparison with other aerosol instruments, *Aerosol Sci. Tech.*, 39(8), 760–770,
976 doi:10.1080/02786820500243404, 2005.

977 Takegawa, N., Miyakawa, T., Kondo, Y., Jimenez, J. L., Zhang, Q., Worsnop, D. R., and Fukuda, M.: Seasonal
978 and diurnal variations of submicron organic aerosol in Tokyo observed using the Aerodyne aerosol
979 mass spectrometer, *J. Geophys. Res.-Atmos.*, 111(D11), D11206, doi:10.1029/2005JD006515,
980 2006.

981 Turpin, B. J. and Lim, H. J.: Species contributions to PM_{2.5} mass concentrations: revisiting common
982 assumptions for estimating organic mass, *Aerosol Sci. Tech.*, 35(1), 602–610,
983 doi:10.1080/02786820152051454, 2001.

984 Turpin, B. J., Saxena, P., and Andrews, E.: Measuring and simulating particulate organics in the
985 atmosphere: problems and prospects, *Atmos. Environ.*, 34(18), 2983–3013, 2000.

986 Ulbrich, I. M., Canagaratna, M. R., Zhang, Q., Worsnop, D. R., and Jimenez, J. L.: Interpretation of organic
987 components from positive matrix factorization of aerosol mass spectrometric data, *Atmos. Chem.*
988 *Phys.*, 9(9), 2891–2918, 2009.

989 Ulbrich, I. M., Lechner, M., and Jimenez, J. L.: AMS Spectral Database, available at:
990 <http://cires.colorado.edu/jimenez-group/AMSsd/> (last access: 7 October 2015), 2015.

991 van Donkelaar, A., Martin, R. V., Brauer, M., Kahn, R., Levy, R., Verduzco, C., and Villeneuve, P. J.: Global
992 estimates of ambient fine particulate matter concentrations from satellite-based aerosol optical
993 depth: development and application, *Environ. Health Persp.*, 118(6), 847–855,
994 doi:10.1289/ehp.0901623, 2010.

995 Volkamer, R., Jimenez, J. L., San Martini, F., Dzepina, K., Zhang, Q., Salcedo, D., Molina, L. T., Worsnop, D.
996 R., and Molina, M. J.: Secondary organic aerosol formation from anthropogenic air pollution: rapid
997 and higher than expected, *Geophys. Res. Lett.*, 33(17), doi:10.1029/2006GL026899, 2006.

998 Watson, J. G., Chow, J. C., Chen, L.-W. A., and Frank, N. H.: Methods to assess carbonaceous aerosol
999 sampling artifacts for IMPROVE and other long-term networks, *J. Air Waste Manage. Assoc.*, 59(8),
1000 898–911, doi:10.3155/1047-3289.59.8.898, 2009.

1001 Weimer, S., Drewnick, F., Högrefe, O., Schwab, J. J., Rhoads, K., Orsini, D., Canagaratna, M., Worsnop, D.
1002 R., and Demerjian, K. L.: Size-selective nonrefractory ambient aerosol measurements during the
1003 particulate matter technology assessment and characterization study - New York 2004 winter
1004 intensive in New York City, *J. Geophys. Res.*, 111(D18), doi:10.1029/2006JD007215, 2006.

1005 WHO: WHO Air quality guidelines for particulate matter, ozone, nitrogen dioxide and sulfur dioxide: global
1006 update 2005: summary of risk assessment, available at:
1007 <http://apps.who.int/iris/handle/10665/69477> (last access: 10 October 2014), 2006.

1008 WHO: Review of evidence on health aspects of air pollution_ REVIHAAP Project, Technical Report,
1009 available at: [http://www.euro.who.int/__data/assets/pdf_file/0004/193108/REVIHAAP-Final-](http://www.euro.who.int/__data/assets/pdf_file/0004/193108/REVIHAAP-Final-technical-report-final-version.pdf)
1010 [technical-report-final-version.pdf](http://www.euro.who.int/__data/assets/pdf_file/0004/193108/REVIHAAP-Final-technical-report-final-version.pdf) (last access: 15 April 2015), 2013.

1011 Wiedensohler, A., Birmili, W., Nowak, A., Sonntag, A., Weinhold, K., Merkel, M., Wehner, B., Tuch, T.,
1012 Pfeifer, S., Fiebig, M., Fjåraa, A. M., Asmi, E., Sellegri, K., Depuy, R., Venzac, H., Villani, P., Laj, P.,
1013 Aalto, P., Ogren, J. A., Swietlicki, E., Williams, P., Roldin, P., Quincey, P., Hüglin, C., Fierz-
1014 Schmidhauser, R., Gysel, M., Weingartner, E., Riccobono, F., Santos, S., Gröning, C., Faloon, K.,
1015 Beddows, D., Harrison, R., Monahan, C., Jennings, S. G., O’Dowd, C. D., Marinoni, A., Horn, H.-G.,
1016 Keck, L., Jiang, J., Scheckman, J., McMurry, P. H., Deng, Z., Zhao, C. S., Moerman, M., Henzing, B.,
1017 de Leeuw, G., Löschau, G., and Bastian, S.: Mobility particle size spectrometers: harmonization of
1018 technical standards and data structure to facilitate high quality long-term observations of
1019 atmospheric particle number size distributions, *Atmos. Meas. Tech.*, 5(3), 657–685,
1020 doi:10.5194/amt-5-657-2012, 2012.

1021 WMO, Zhu, T., Melamed, M., Parrish, D., Gauss, M., Gallardo Klenner, L., Lawrence, M., Konare, A., and
1022 Liousse, C.: WMO/IGAC impacts of megacities on air pollution and climate, available at:

1023 http://www.igacproject.org/sites/all/themes/bluemasters/images/GAW_Report_205.pdf (last
1024 access: 29 July 2015), 2012.

1025 Young, D. E., Allan, J. D., Williams, P. I., Green, D. C., Harrison, R. M., Yin, J., Flynn, M. J., Gallagher, M. W.,
1026 and Coe, H.: Investigating a two-component model of solid fuel organic aerosol in London:
1027 processes, PM₁ contributions, and seasonality, *Atmos. Chem. Phys.*, 15(5), 2429–2443,
1028 doi:10.5194/acp-15-2429-2015, 2015.

1029 Zhang, Q.: Time- and size-resolved chemical composition of submicron particles in Pittsburgh: implications
1030 for aerosol sources and processes, *J. Geophys. Res.*, 110(D7), doi:10.1029/2004JD004649, 2005.

1031 Zhang, Q., Jimenez, J. L., Canagaratna, M. R., Allan, J. D., Coe, H., Ulbrich, I., Alfarra, M. R., Takami, A.,
1032 Middlebrook, A. M., Sun, Y. L., Dzepina, K., Dunlea, E., Docherty, K., DeCarlo, P. F., Salcedo, D.,
1033 Onasch, T., Jayne, J. T., Miyoshi, T., Shimojo, A., Hatakeyama, S., Takegawa, N., Kondo, Y.,
1034 Schneider, J., Drewnick, F., Borrmann, S., Weimer, S., Demerjian, K., Williams, P., Bower, K.,
1035 Bahreini, R., Cottrell, L., Griffin, R. J., Rautiainen, J., Sun, J. Y., Zhang, Y. M., and Worsnop, D. R.:
1036 Ubiquity and dominance of oxygenated species in organic aerosols in anthropogenically-
1037 influenced Northern Hemisphere midlatitudes, *Geophys. Res. Lett.*, 34(13),
1038 doi:10.1029/2007GL029979, 2007.

1039 Zhang, Q., Jimenez, J. L., Canagaratna, M. R., Ulbrich, I. M., Ng, N. L., Worsnop, D. R., and Sun, Y.:
1040 Understanding atmospheric organic aerosols via factor analysis of aerosol mass spectrometry: a
1041 review, *Anal. Bioanal. Chem.*, 401(10), 3045–3067, doi:10.1007/s00216-011-5355-y, 2011.

1042 **Tables and Figures**

1043

1044 Table 1. Consistency of ACSM measurements: comparison between ACSM and independent analytical techniques using orthogonal regression
 1045 analyses. Slopes and intercepts are indicated \pm uncertainties.

1046

	r^2					slope					intercept				
	Sp	Su	Au	Wi	An	Sp	Su	Au	Wi	An	Sp	Su	Au	Wi	An
Org vs OC	0.91	0.90	0.86	0.92	0.77	2.18 ± 0.07	2.92 ± 0.10	1.87 ± 0.09	1.26 ± 0.04	1.72 ± 0.04	-0.29 ± 0.37	-1.07 ± 0.32	-0.28 ± 0.36	0.74 ± 0.37	0.61 ± 0.25
Nitrate	0.95	0.53	0.96	0.92	0.91	1.37 ± 0.03	4.27 ± 0.25	1.28 ± 0.03	0.86 ± 0.03	1.28 ± 0.02	0.42 ± 0.18	0.64 ± 0.11	0.48 ± 0.10	0.62 ± 0.11	0.48 ± 0.09
Sulfate	0.96	0.97	0.92	0.86	0.95	1.05 ± 0.02	0.98 ± 0.02	0.96 ± 0.04	1.38 ± 0.06	1.00 ± 0.01	-0.01 ± 0.04	0.02 ± 0.06	0.04 ± 0.07	-0.25 ± 0.06	0.00 ± 0.03
Ammonium	0.92	0.70	0.91	0.95	0.90	1.03 ± 0.03	1.00 ± 0.06	0.93 ± 0.04	0.81 ± 0.02	0.99 ± 0.02	-0.04 ± 0.07	-0.04 ± 0.07	-0.12 ± 0.05	0.03 ± 0.03	-0.08 ± 0.03
Chloride	0.75	0.00	0.59	0.78	0.52	2.68 ± 0.13	-0.13 ± 0.09	0.68 ± 0.06	1.13 ± 0.07	1.75 ± 0.06	0.04 ± 0.01	0.03 ± 0.00	0.04 ± 0.00	-0.02 ± 0.01	0.02 ± 0.01
Mass vs volume	0.87	0.82	0.88	0.85	0.81	1.91 ± 0.01	1.95 ± 0.02	1.45 ± 0.01	1.34 ± 0.01	1.63 ± 0.01	-1.16 ± 0.19	-1.36 ± 0.18	-2.45 ± 0.19	-0.11 ± 0.20	-1.09 ± 0.11

1047

1048

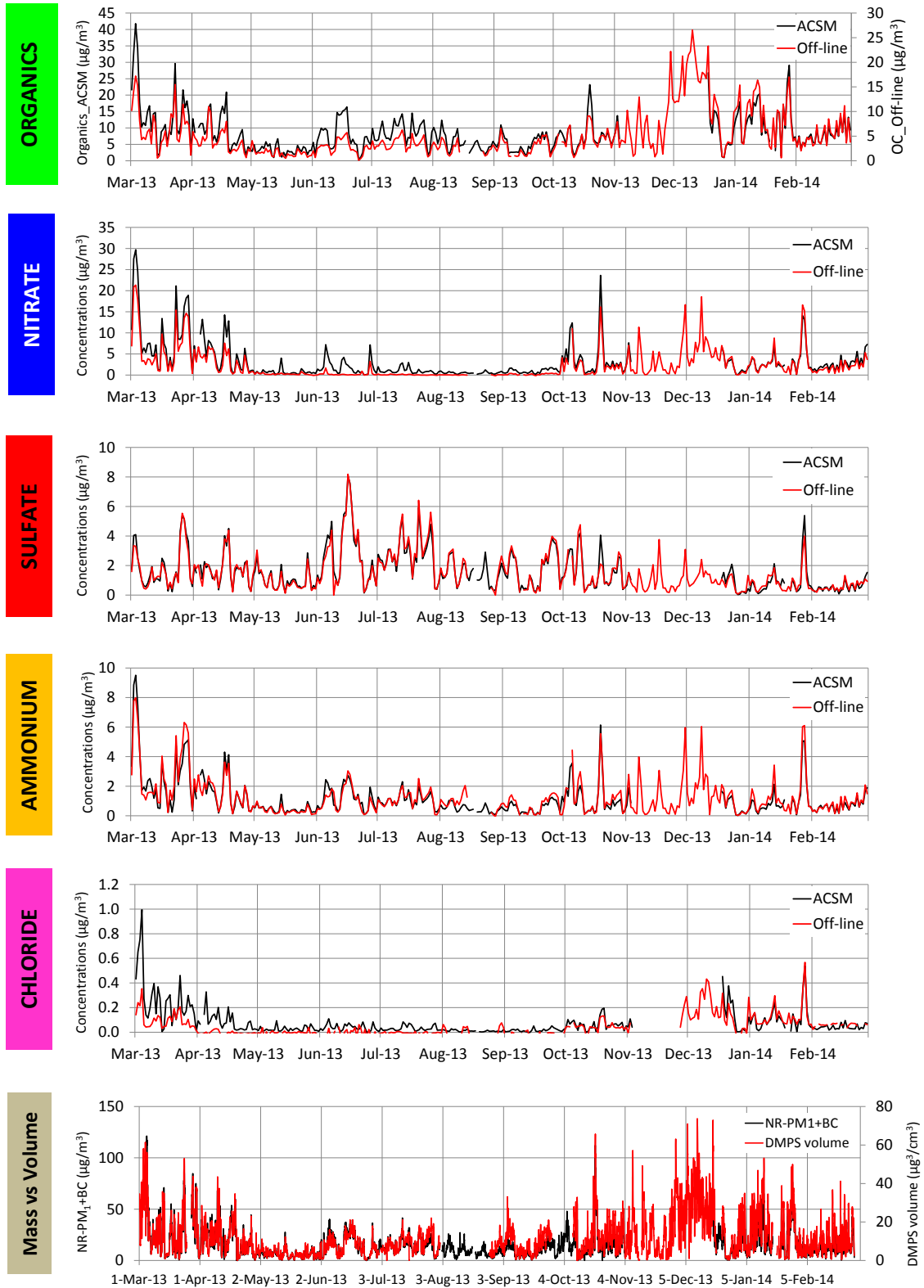
1049 Legend: Sp: spring (March-April-May), Su: summer (June-July-August), Au: autumn (September-October-November), Wi: winter (December-
 1050 January-February), An: annual. Independent analytical techniques refer to i) EC-OC Sunset Analyzer for OC from PM_{2.5} sampling, ii) Ion
 1051 Chromatography for ions from PM_{2.5} sampling and iii) DMPS for volume concentrations (see Sect. 2.3 for more details). Mass refers to NR-PM₁+BC.
 1052 Intercepts are in $\mu\text{g}/\text{m}^3$. Slopes of mass vs volume are in g/cm^3 and dimensionless otherwise.

1053 Table 2. Comparison (coefficient of determination, r^2) between SA factors, organic m/z tracers and independent species time series. BC stands
 1054 for Black Carbon; Org_i stands for organic signal at m/z i (i=43, 44, 60, 67, 73, 81).

1055

	HOA					BBOA					OOA				
	Org_67	Org_81	NOx	CO	BC	Org_60	Org_73	NOx	CO	BC	Org_43	Org_44	NH4	SO4	NO3
SPRING	0.60	0.55	0.03	0.08	0.28	0.99	0.97	0.32	0.81	0.70	0.88	0.94	0.76	0.43	0.77
SUMMER	0.90	0.91	0.07	0.40	0.52			-			0.97	0.94	0.54	0.60	0.19
AUTUMN	0.63	0.61	0.07	0.10	0.24	0.99	0.97	0.06	0.68	0.47	0.82	0.92	0.47	0.53	0.38
WINTER	0.58	0.57	0.34	0.33	0.39	0.98	0.97	0.20	0.66	0.63	0.80	0.99	0.50	0.39	0.66

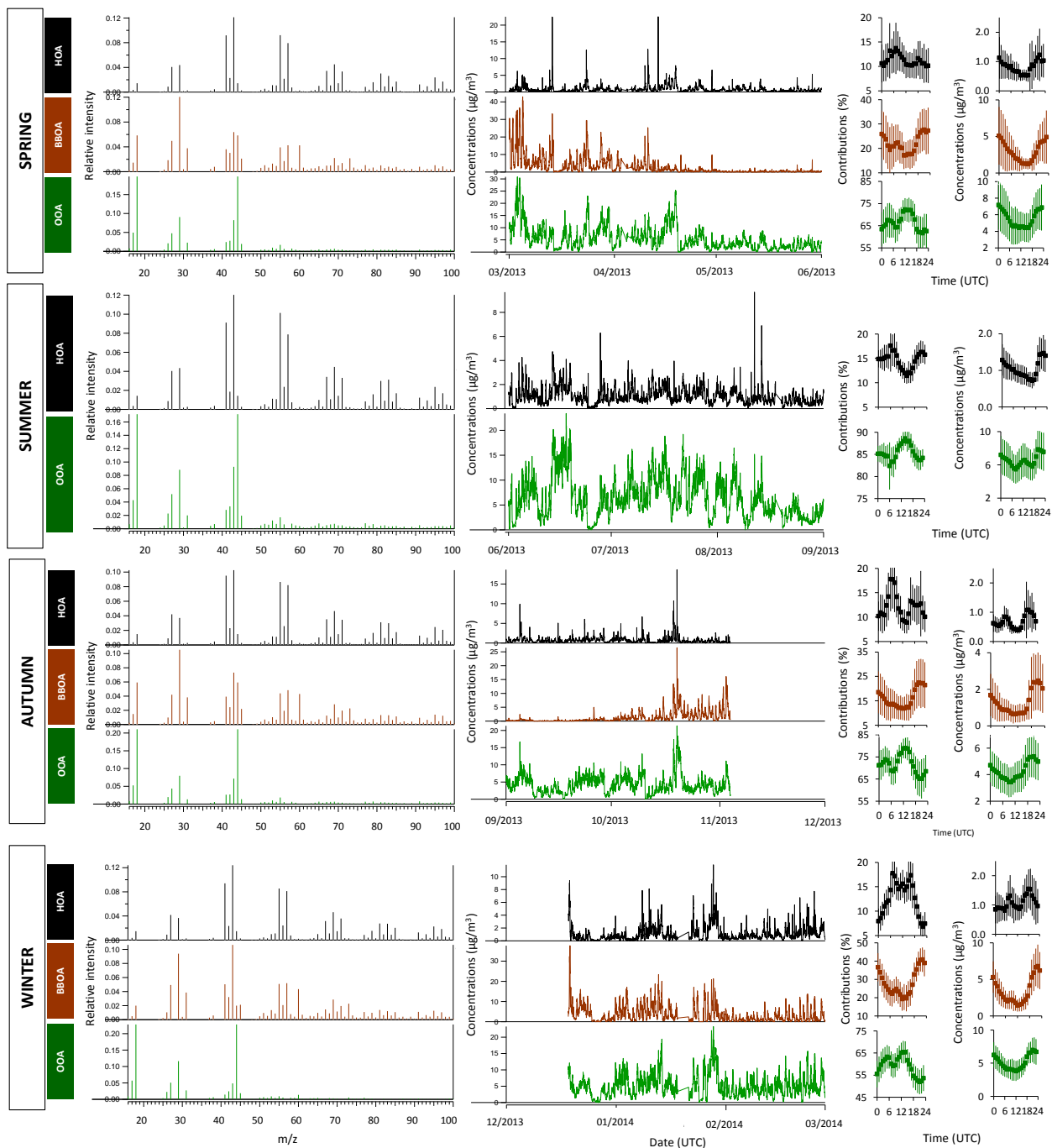
1056



1057

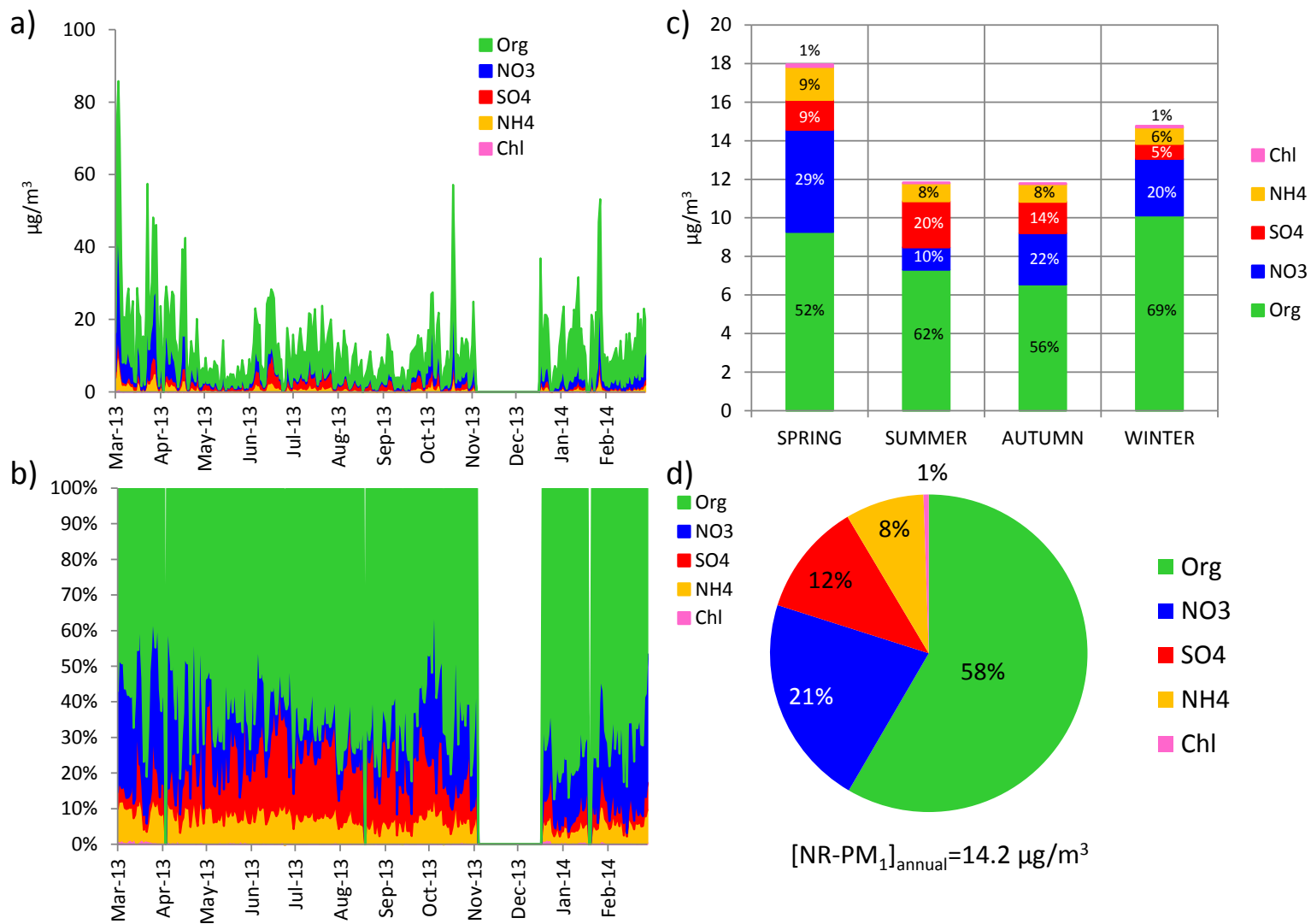
1058 Figure 1. Comparison between measurements performed with the ACSM and other co-located analytical

1059 techniques. See Table 1 and Sect. 2.3 for more details.



1060

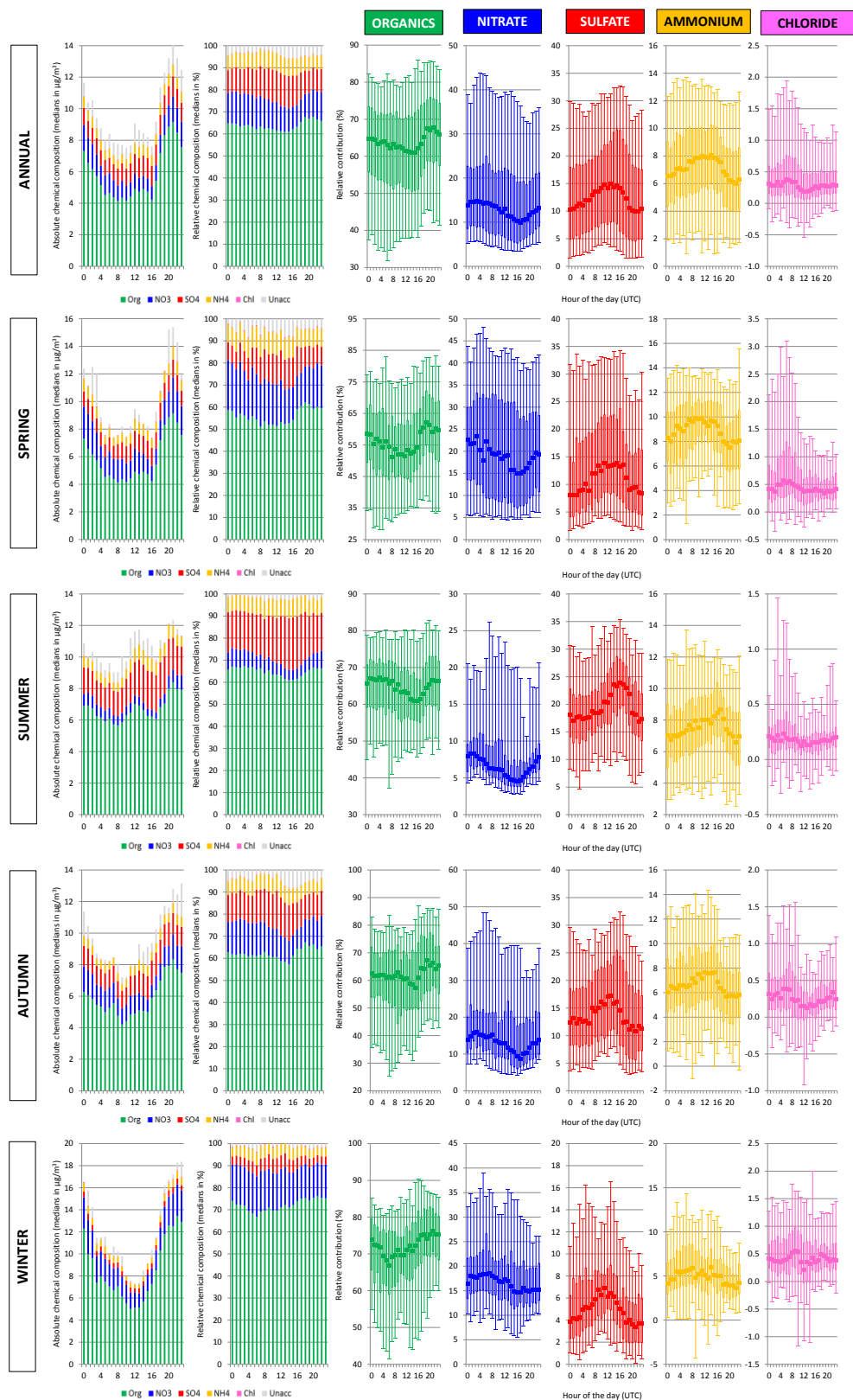
1061 Figure 2. Organic source apportionment presented by season: factor profiles (left), time series (middle)
 1062 and daily cycles (right, error bars represent 1 standard deviation). Seasons are defined as Spring: MAM,
 1063 Summer: JJA, Autumn: SON and Winter: DJF.



1064

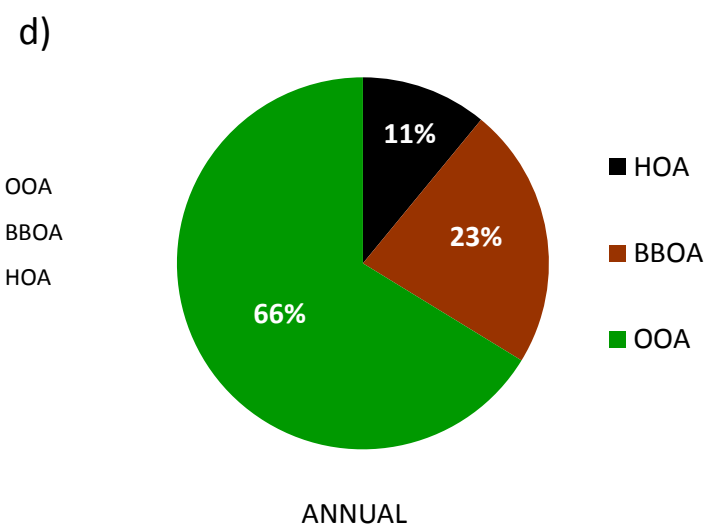
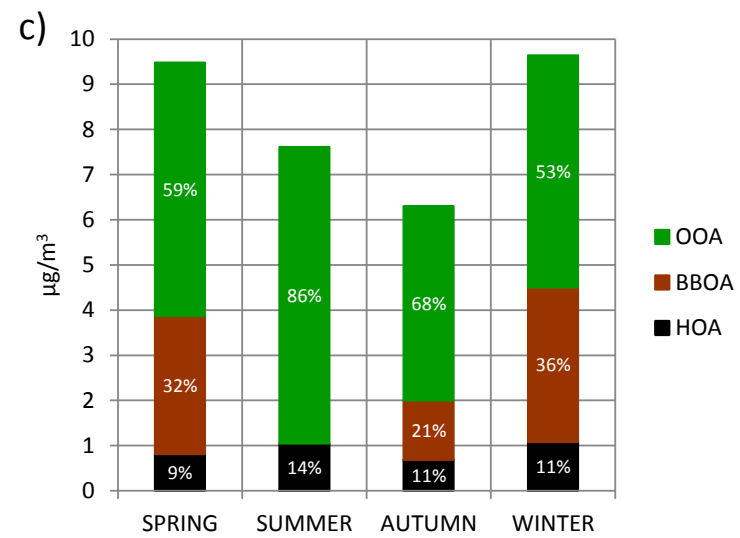
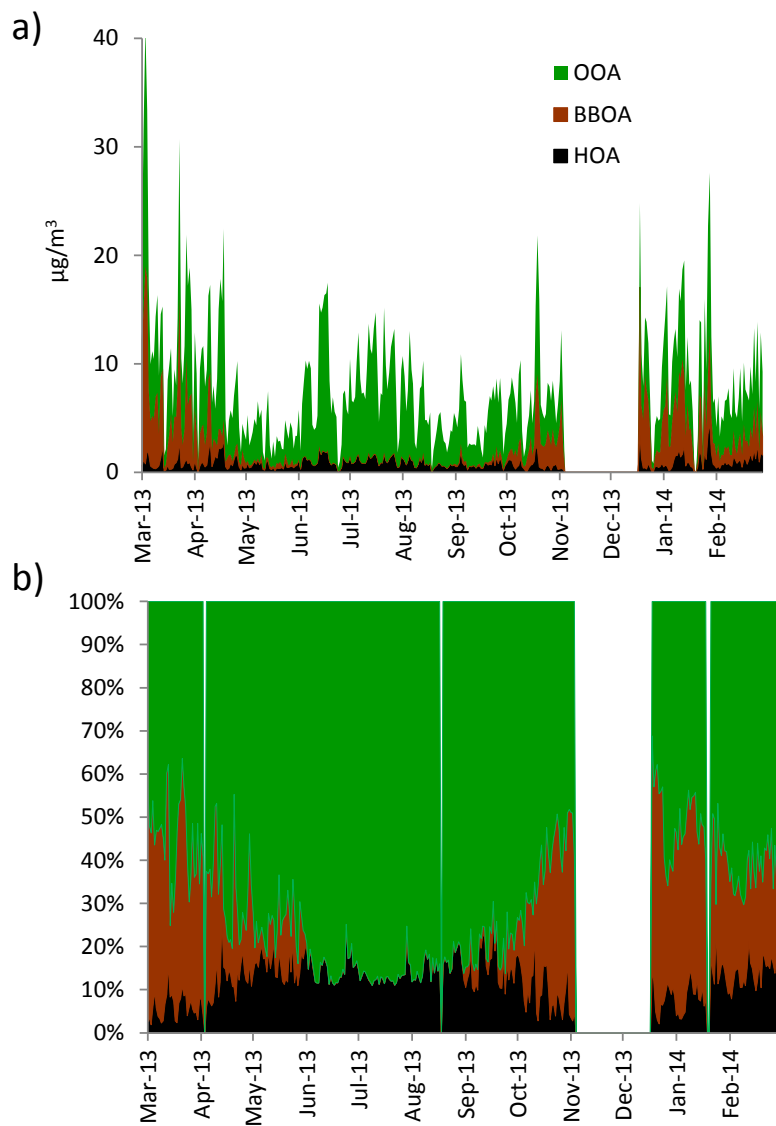
1065 Figure 3. Overview of the chemical composition of NR-PM₁ at Ispra (Po Valley, Italy): daily absolute (a) and relative (b) chemical composition;

1066 seasonal (c) and annual (d) averages.



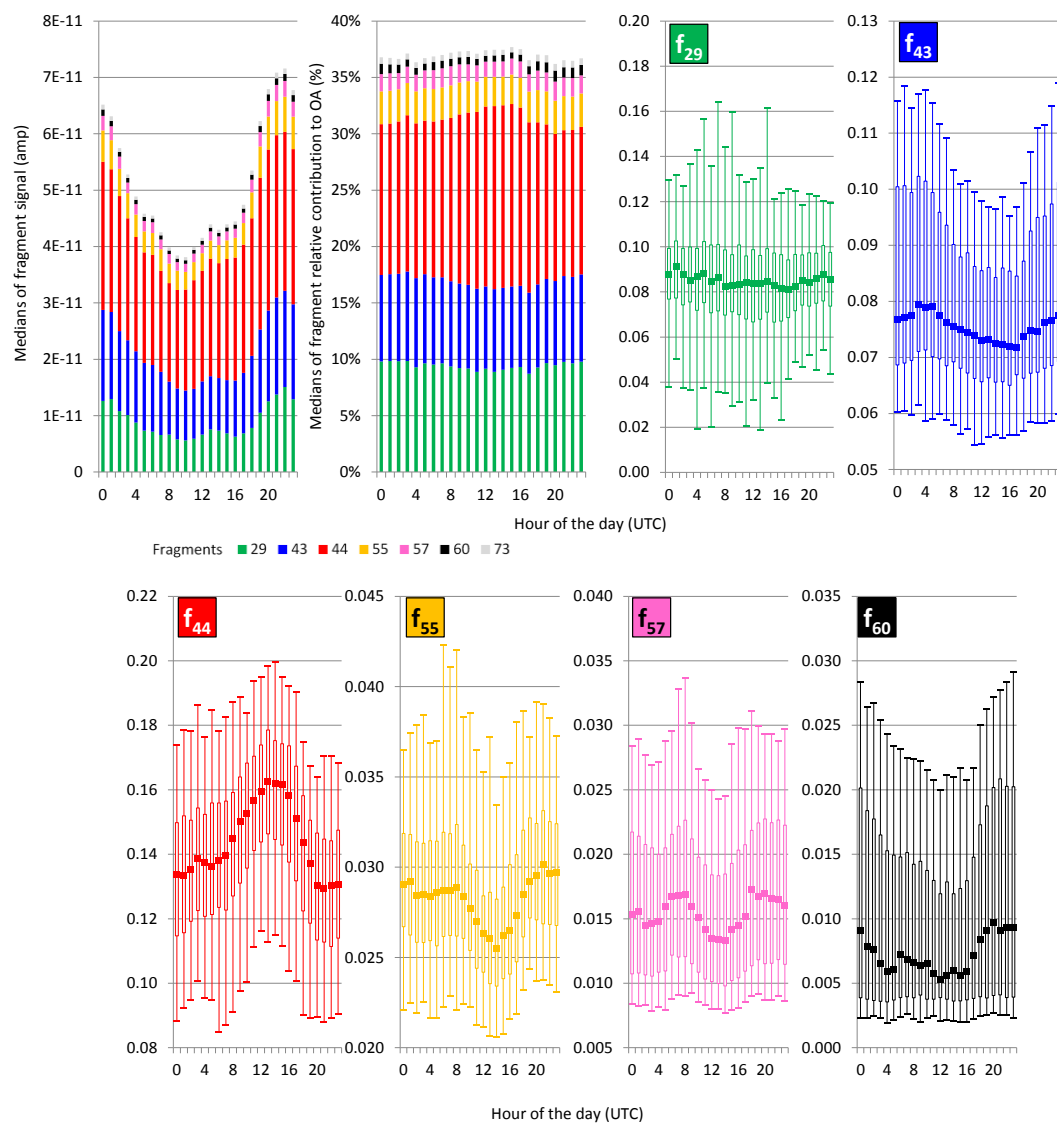
1067

1068 Figure 4. Daily cycles of NR-PM₁ chemical composition on the annual and seasonal scales. Unacc:
 1069 unaccounted mass, whisker plots are constructed from the 5th, 25th, 50th, 75th and 95th percentiles.



1070

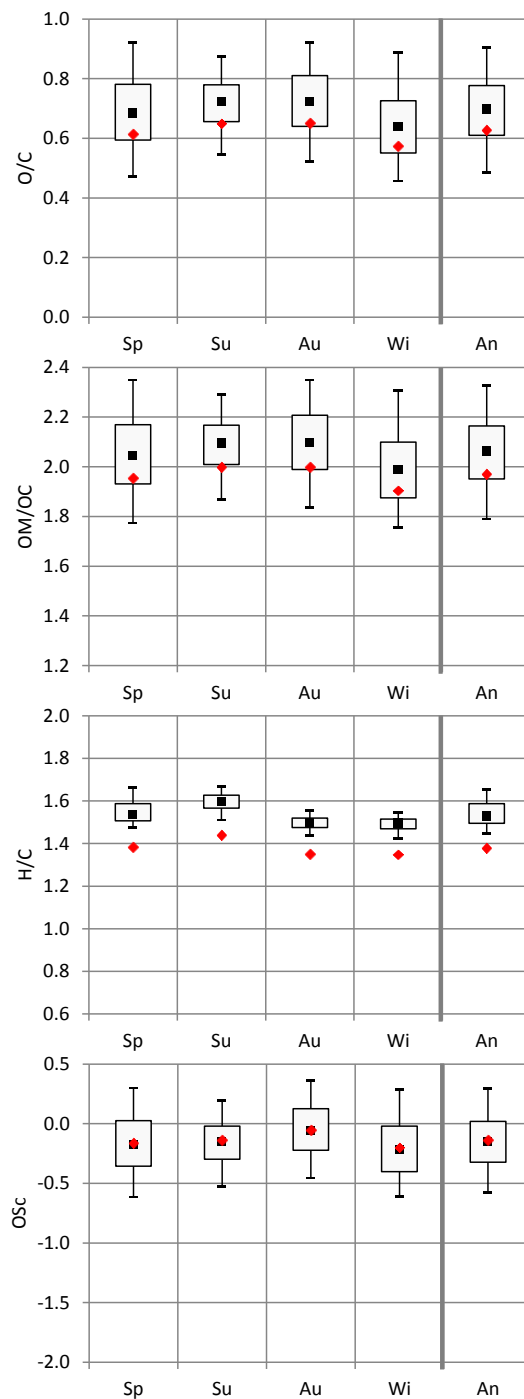
1071 Figure 5. Overview of HOA, BBOA and OOA contributions to organic aerosols; see legend Figure 3.



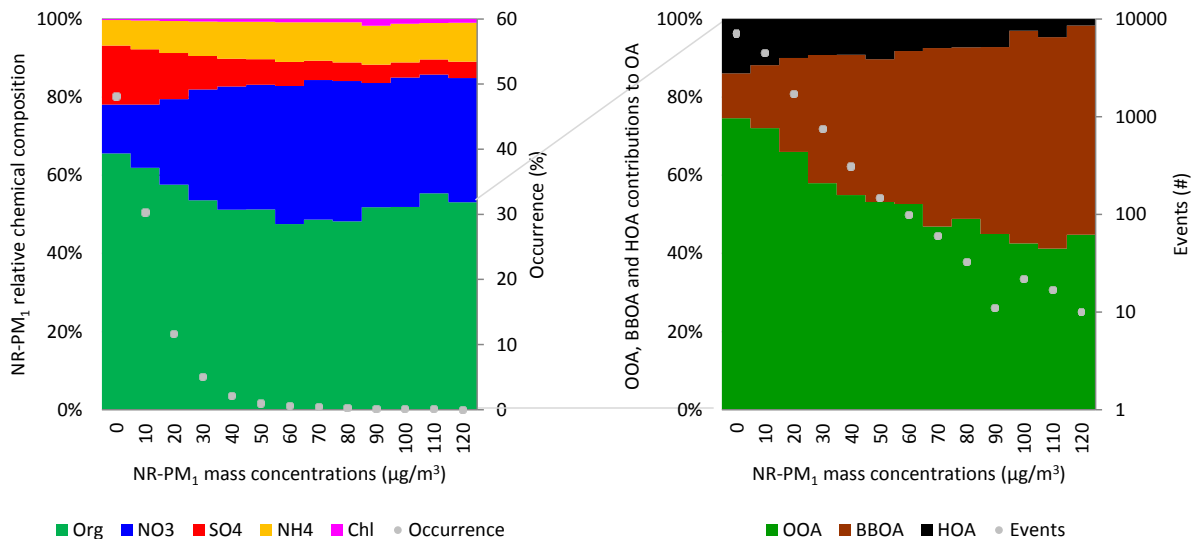
1072

1073 Figure 6. Annual statistics describing the daily cycles of the major organic fragments. Box plots are constructed from the 5th, 25th, 50th, 75th and

1074 95th percentiles.



1075
 1076 Figure 7. Seasonal and annual O/C, OM/OC, H/C and OSc of ambient OA. Sp: spring (MAM), Su: summer
 1077 (JJA), Au: autumn (SON), Wi: winter (DJF), An: annual. Black: 5th, 25th, 50th, 75th and 95th percentiles
 1078 estimates following Canagaratna et al. (2015); red: median estimates following Aiken et al. (2008) for O/C
 1079 and OM/C, Ng et al. (2011b) for H/C and Aiken et al. (2008), Kroll et al. (2011) and Ng et al. (2011b) for
 1080 OSc. Note that the authors do not recommend comparing absolute O/C, OM/OC and OSc values reported
 1081 here with other AMS studies, given the uncertainties associated with f_{44} quantifications from ACSM
 1082 measurements (please see text).



1083

1084 Figure 8. NR-PM₁ relative chemical composition (left) and OA factor contributions (right) averages in
 1085 function of NR-PM₁ mass concentrations (bins of 10 µg/m³). Occurrence (% , left) and number of events
 1086 (#, right) are indicated (solid dots) for each NR-PM₁ bin. Note that one event corresponds to one 30 minute
 1087 average.